相対論数学との出会い

佐藤文隆（京大名誉教授）

前半では一般相対論が宇宙物理の観測的発見で“流行り”になった歴史話をして、後半で自分の一般相対論経験を話す。

A 1963年にRelativistic Astrophysicsという研究が始まったが、重力崩壊も膨張宇宙も一般相対論は球対称と線形重力波なのでニュートン重力の物理的直観で済んだ。

B 非球対称に踏み出した1970年前後、その時に見えた一般相対論研究の印象を話し

C最後に自分が取り組んだ
「TS解」[1][2]、
「計量テンソルの張り合わせ」[3]、
「一様空間のトポロジー」[4]などについて話す。

[1]H Sato and A Tomimatsu “Multi-soliton Solution of the Einstein Equation and Tomimastu-Sato Metric” Prog. Theor. Phys.Supplement No 70(1981),215-237.
[2]V S Manko “On the Physical Interpretation of δ = 2 Tomimatsu-Sato Solution” Prog. Theor. Phys. 127(2012),1057.
[3]H Sato “Motion of Shell at Metric Junction”, Prog. Theor. Phys.76(1986),1250-1259.
[4]前田恵一『宇宙のトポロジー』岩波書店 1999年。

A　「不毛」だが魅惑の一般相対論　　量子力学１００

・パウリのハイゼンベルグへの忠告
・切り取られたページ
・１９３９年Oppenheimer-Volkov 、Oppenheimer-Snyder　原爆４２－４５
・統一理論　KK理論、幾何の拡張、多次元、矢野健太郎、波動幾何
・一般相対論の量子化　ハミルトン形式3+1　内山龍雄「隠れてやる」

B　宇宙観測の発見で突然一般相対論がブームに

・電波天文　干渉系　星のように分解できない天体　赤方偏移　小さくてて巨大エネルギー
・レーダー　マイクロ波　人工衛星　通信衛星　残るノイズ　背景放射　CMBの発見
・電離層変動電波　パルサー発見
・Weber 重力波検出　Weber　→ X
・太陽ニュートリノ　Dives
・X線星
・γ線バースト

Lyle　星のように分解できない天体

　　－－＞quasar

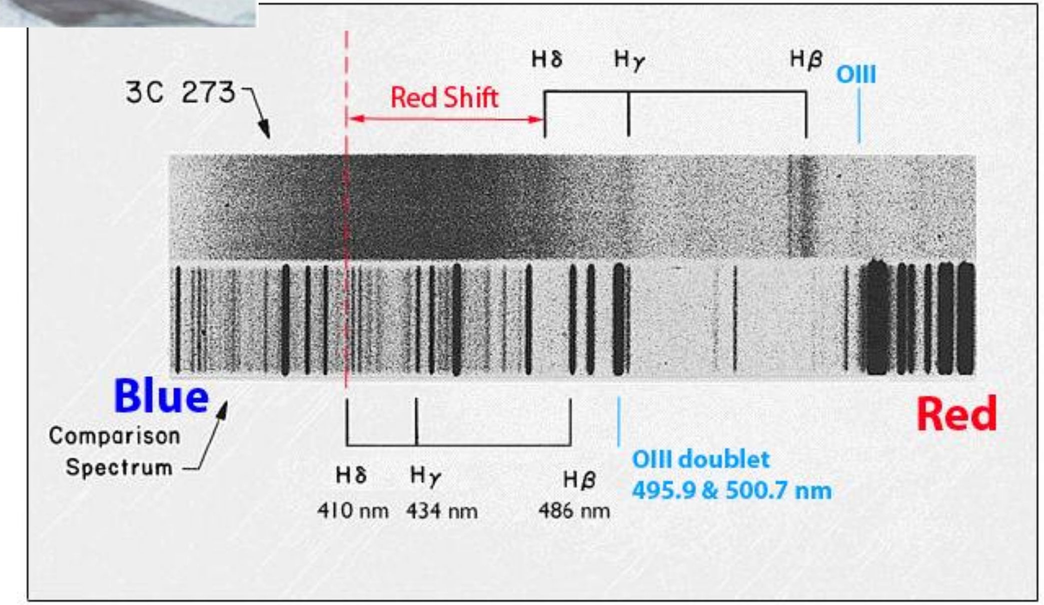

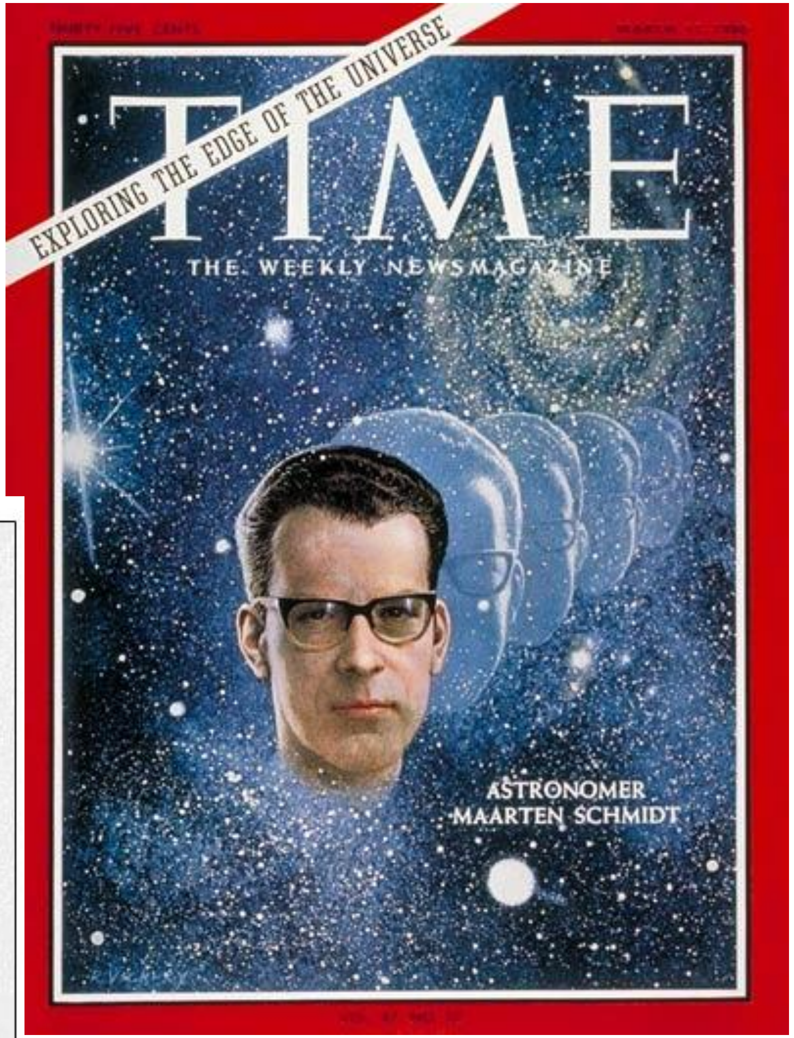

1966

HFBB論文 “ On Relativistic Astrophysics”

Astrophysical Journal, vol. 139, p.909,April,1964

テキサス・シンポジューム　１９６３

Preprint. 林研のコロキュウムで紹介
1939年Oppenheimer-Snyder 論文紹介

湯川秀樹やってくる

1962年春　Wheeler講義　林憲二、白藤・・

先輩、同僚皆無、　　文献 基礎研図書室

1963 QSO. HFBB

1965 CMB発見

1966 PhD　超重量星

1967 ビッグバン元素

宇宙の晴れ上がり、原始水素分子、銀河形成・・・

1971　基礎物理学研究所助教授

一般相対論

素粒子宇宙　反物質TS

1972 TS解

1973年9月　Solvey Conference　重力と宇宙論

Wheeler
Trautman
Schild
Newman
Ruffini
Gold

Prigogin

1973 Solvay Conf

1975. Tomimatsu-Sato
Cambridge-UK
1947-12

一般相対論研究の[火種]

Schwarzschild,de-Sitter,Freedman,Lemaitre,Toleman

Miln,Bondi,Sciama, Robinson. -->
Penrose,Israel,Ellis,Hawking, MaCallum,Gibbons
Jordan->Ehlers,Kundt,Sacks,Schucking,
Schild->Kerr
Wheeler->Misner,Thorne,Ruffini,Hartle,Wald,Unrhu,
Infeld ->Bergman,Trautman
Landau-Lifshitz->Khalatonikov,Belinsky,
Chandra ->Gerosh,Kinnersly
Zeldovich->Novikov.Sunyaev

Petrov分解　　－＞Kerr-Schild、Peeling Theorem

Bianchiタイプ、Taub-NUT、BKL

Newmann-Penrose Spinor

大域構造　　Penroseダイアグラム　Krsukal

２-Killing vectors、 Ernst 方程式

Raychudri Eq－＞特異点定理.

宇宙検閲仮説－＞event horizon、Kerr唯一解

ゲージ不変摂動

一般相対論研究の勉強

見えてきたもの

Petrov分類　**Weylテンソル**　**露**

Bianchiタイプ　**伊**

Raychaudhuri方程式　**印**

大域的、N-P

$\{z_1, z_2, z_3, z_4\}$. Then the Petrov types can be defined as follows:

$$\begin{cases} \textbf{Type O} & \rightarrow \text{ Weyl tensor is zero} \\ \textbf{Type I} & \rightarrow \text{ All roots are different} \\ \textbf{Type D} & \rightarrow \text{ Two pairs of roots coincide, } z_1 = z_2 \neq z_3 = z_4 \\ \textbf{Type II} & \rightarrow \text{ Two roots coincide, } z_1 = z_2 \neq z_3 \neq z_4 \neq z_1 \\ \textbf{Type III} & \rightarrow \text{ Three roots coincide, } z_1 = z_2 = z_3 \neq z_4 \\ \textbf{Type N} & \rightarrow \text{ All roots coincide, } z_1 = z_2 = z_3 = z_4 \,. \end{cases} \tag{2.15}$$

These four roots define four Lorentz transformations. By means of eq. (2.13) such transformations lead to four privileged null vector fields $\boldsymbol{l}'_i$, which are the ones obtained by performing these transformations on the vector field $\boldsymbol{l}$ of the original null tetrad:

$$\boldsymbol{l} \rightarrow \boldsymbol{l}'_i = \boldsymbol{l} + \overline{z_i}\,\boldsymbol{m} + z_i\,\overline{\boldsymbol{m}} + |z_i|^2\,\boldsymbol{n}\,, \quad i \in \{1, 2, 3, 4\}\,. \tag{2.16}$$

null infinity. Let γ be a null geodesic in a spacetime (M, g_{ab}) from a point p

parameter λ. Then the theorem states that, as λ tends to infinity:

$$C_{abcd} = \frac{C^{(1)}_{abcd}}{\lambda} + \frac{C^{(2)}_{abcd}}{\lambda^2} + \frac{C^{(3)}_{abcd}}{\lambda^3} + \frac{C^{(4)}_{abcd}}{\lambda^4} + O\left(\frac{1}{\lambda^5}\right)$$

where C_{abcd} is the Weyl tensor, and abstract index notation is used. Moreover $C^{(1)}_{abcd}$ is type N, $C^{(2)}_{abcd}$ is type III, $C^{(3)}_{abcd}$ is type II (or II-II) and $C^{(4)}_{abcd}$ is type I.

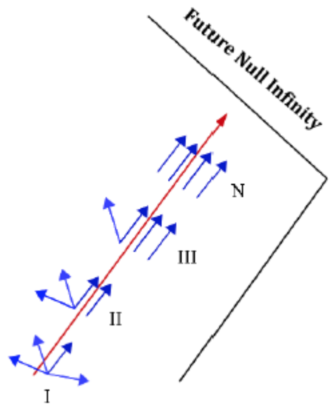

Figure 3.3: According to the peeling theorem, as we approach the null infinity of an asymptotically flat space-time the Petrov type of the Weyl tensor becomes increasingly special. The blue arrows represent the principal null directions of the Weyl tensor, while the red axis represents the null direction along which null infinity is approached.

$$\dot{\theta} = -\frac{\theta^2}{3} - 2\sigma^2 + 2\omega^2 - E[\vec{X}]^a{}_a + \dot{X}^a{}_{;a}$$

ここで、

$$\sigma^2 = \frac{1}{2}\sigma_{mn}\,\sigma^{mn},\ \omega^2 = \frac{1}{2}\omega_{mn}\,\omega^{mn}$$

は、それぞれ剪断応力テンソル

$$\sigma_{ab} = \theta_{ab} - \frac{1}{3}\,\theta\,h_{ab}$$

および渦度テンソル

$$\omega_{ab} = h^m{}_a\,h^n{}_b X_{[m;n]}$$

の（非負の）二次不変量である。また、

$$\theta_{ab} = h^m{}_a\,h^n{}_b X_{(m;n)}$$

は膨張テンソル、 θ はそのトレース で膨張スカラーと呼ばれるもの、そして

$$h_{ab} = g_{ab} + X_a\,X_b$$

は $\vec{X}$ に直交する超平面への射影テンソルである。また、ドットは合同内の世界線の固有時による微分を表わす。 $E[\vec{X}]_{ab}$ のトレースは次のようにも書ける。

$$E[\vec{X}]^a{}_a = R_{mn}\,X^m\,X^n$$

Varenna Como湖

Fermi-summer-Schoole

1975

１９８３年

１９８４年

１９８５年

白藤、Hoenserales,松下

Ernst,Penrose,　X,　Ehlers

Macllum


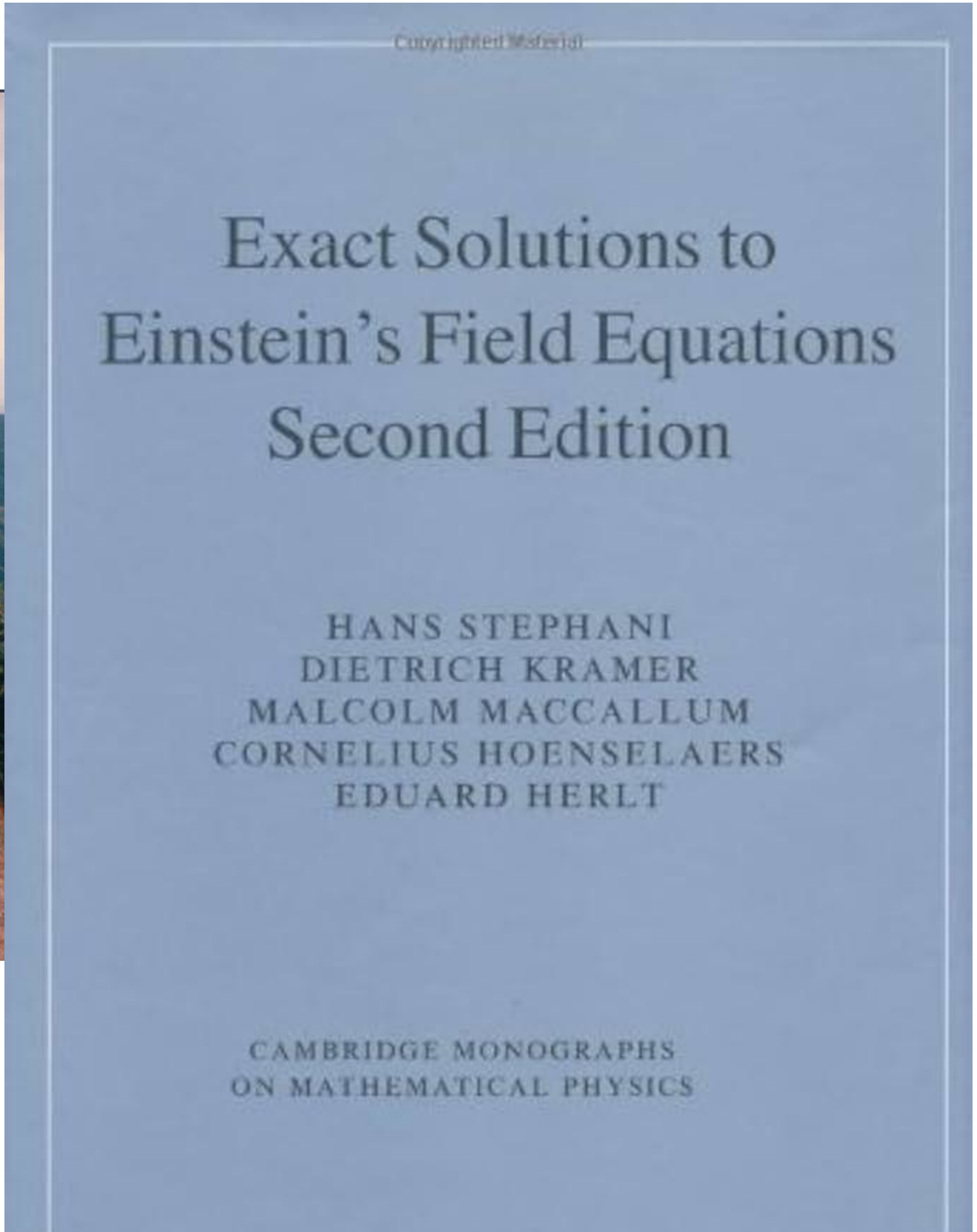
Copyrighted Material
Exact Solutions to
Einstein's Field Equations
Second Edition
HANS STEPHANI
DIETRICH KRAMER
MALCOLM MACCALLUM
CORNELIUS HOENSELAERS
EDUARD HERLT
CAMBRIDGE MONOGRAPHS
ON MATHEMATICAL PHYSICS

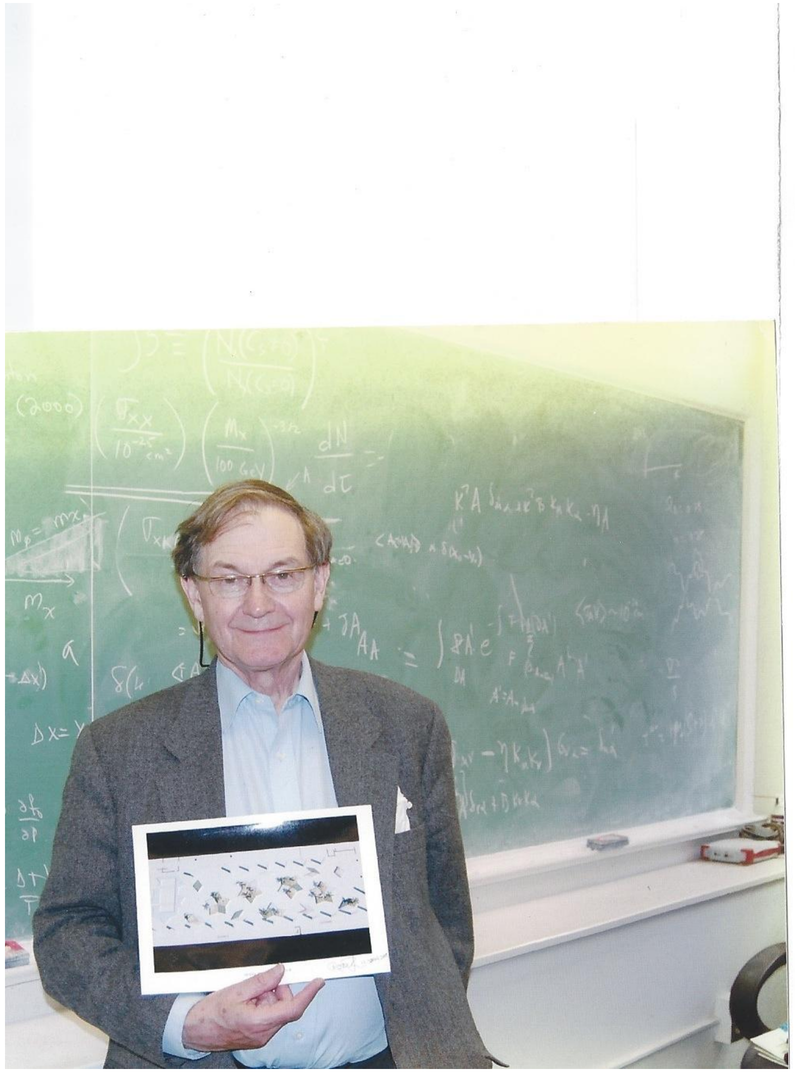

Dear Professor Sato

Greeting from

New York —

and best wishes

Roger

Werner, Inge Israel
Silk

石原
Khalatonikov
Belinsky
Sato
Kodama

Kerr

Trautman

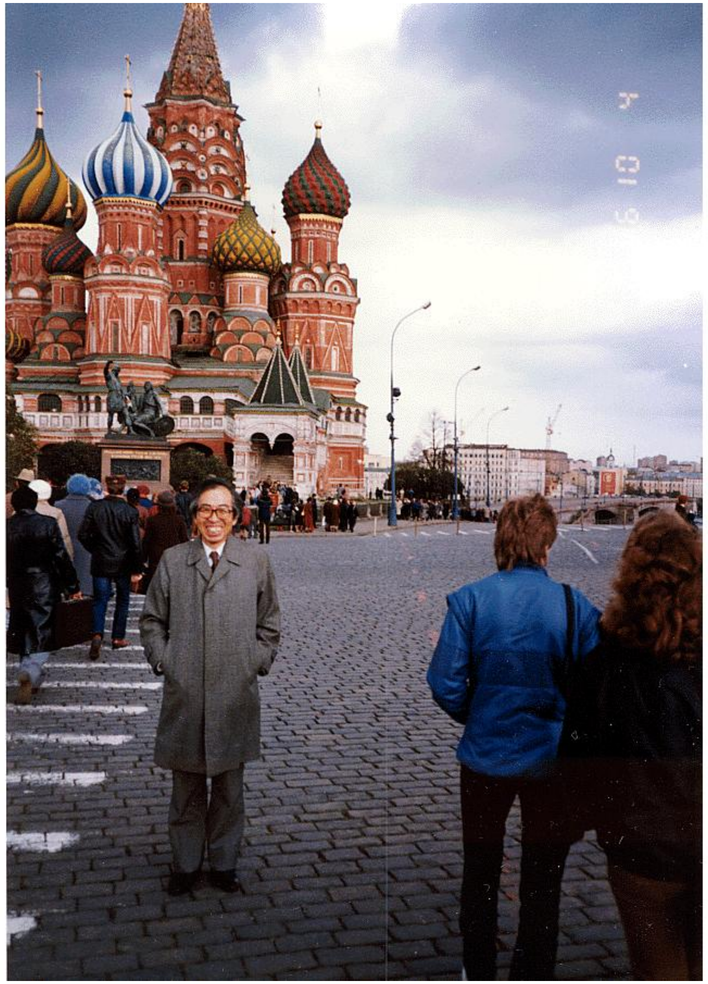

Logonov
周培源
Vaidya

一般相対論　vs.　重力

Newton　　　運動　＋　力　＋時空

Maxwell. 力＋[特殊]相対論　Lorentz-Einstein-Minkowski

Einstein. 一般相対論＝＞局所慣性系（M)の[一般]変換

＝＞　たかが「見方の選択」慣性系の実体性、「敗れ」

Fermi-Walker tetrad

三つの{量子}力＝標準理論.

ゲージ理論（対称性の接続）

Lorentz対称性の一般座標変換

のゲージ理論

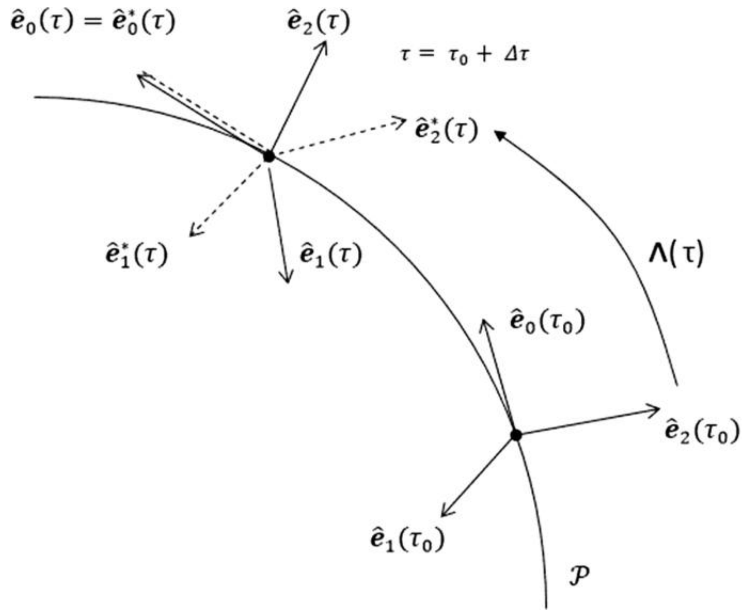

調和写像

M の局所座標系 (x^i) および N の局所座標系 (y^α) のもとで，M と N の Riemann 計量 g と h はそれぞれ

$$g = \sum_{i,j=1}^{m} g_{ij} dx^i dx^j, \quad h = \sum_{\alpha,\beta=1}^{n} h_{\alpha\beta} dy^\alpha dy^\beta$$

と表示され，写像 f は

$$f(x) = \big(f^1(x^1, \ldots, x^m), \ldots, f^n(x^1, \ldots, x^m)\big) = \big(f^\alpha(x^i)\big)$$

とあらわすことができる．このとき

$$e(f) = |df|^2 = \mathrm{Trace}_g f^* h = \sum_{i,j=1}^{m} \sum_{\alpha,\beta=1}^{n} g^{ij} h_{\alpha\beta}(f) \frac{\partial f^\alpha}{\partial x^i} \frac{\partial f^\beta}{\partial x^j}$$

で定義される C^∞ 級関数 $e(f) : M \to \boldsymbol{R}$ を f のエネルギー密度 (energy density) といい，M 上で $e(f)$ を積分した値

揺らぐ一般相対論
量子、　　　宇宙モデル、・・

曲がった時空での量子場、加速度放射
多様体　連続　vs　量子　離散
古典論の限界

弦集団　　　の
　熱力学的理論
　entropic force

Tomimatsu-Sato metric

A　解の生成法

B　時空構造

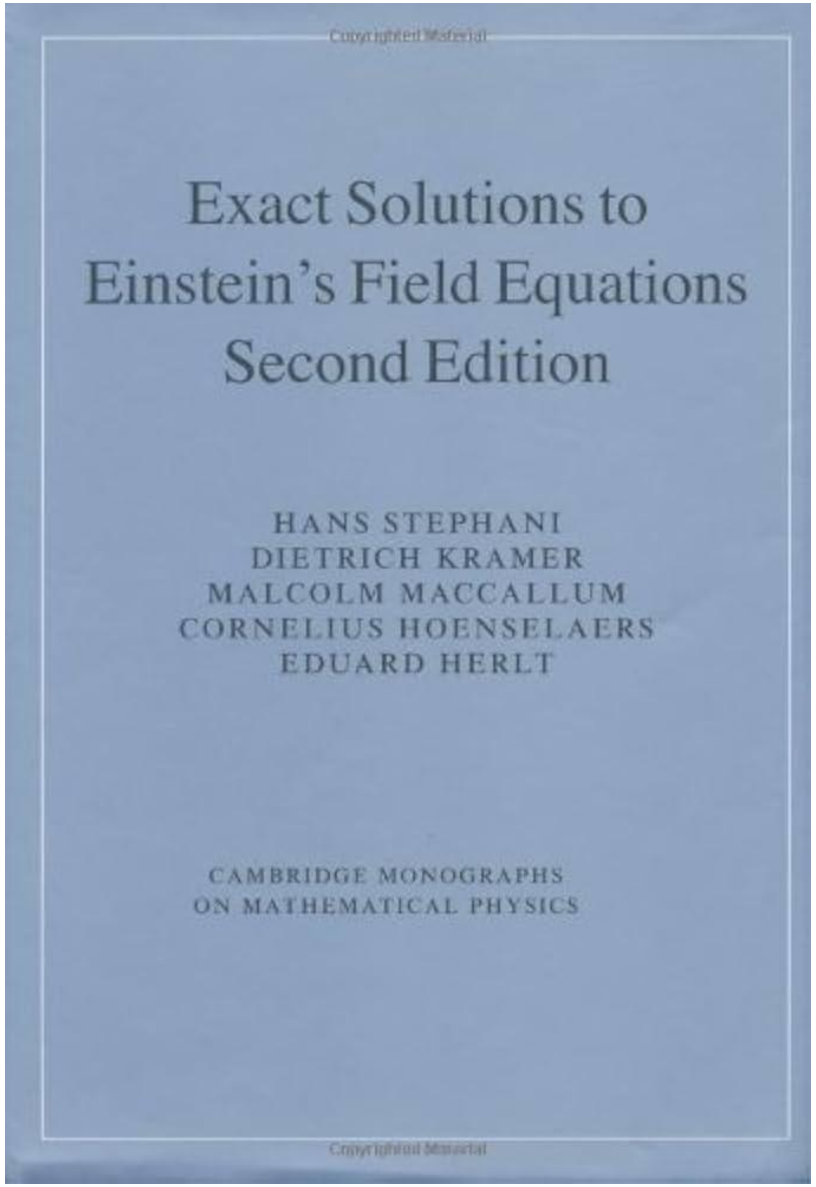

Stephani,
Kramers,
Maccallum,
Hoenserales,
Hert

Cambridge UP 2nd 2002

V S Manko “On the Physical Interpretation of $\delta = 2$ Tomimatsu-Sato Solution” Prog. Theor. Phys. 127(2012),1057

The Tomimatsu-Sato metric reloaded

D. Batic*

http://arxiv.org/abs/2302.11888v1

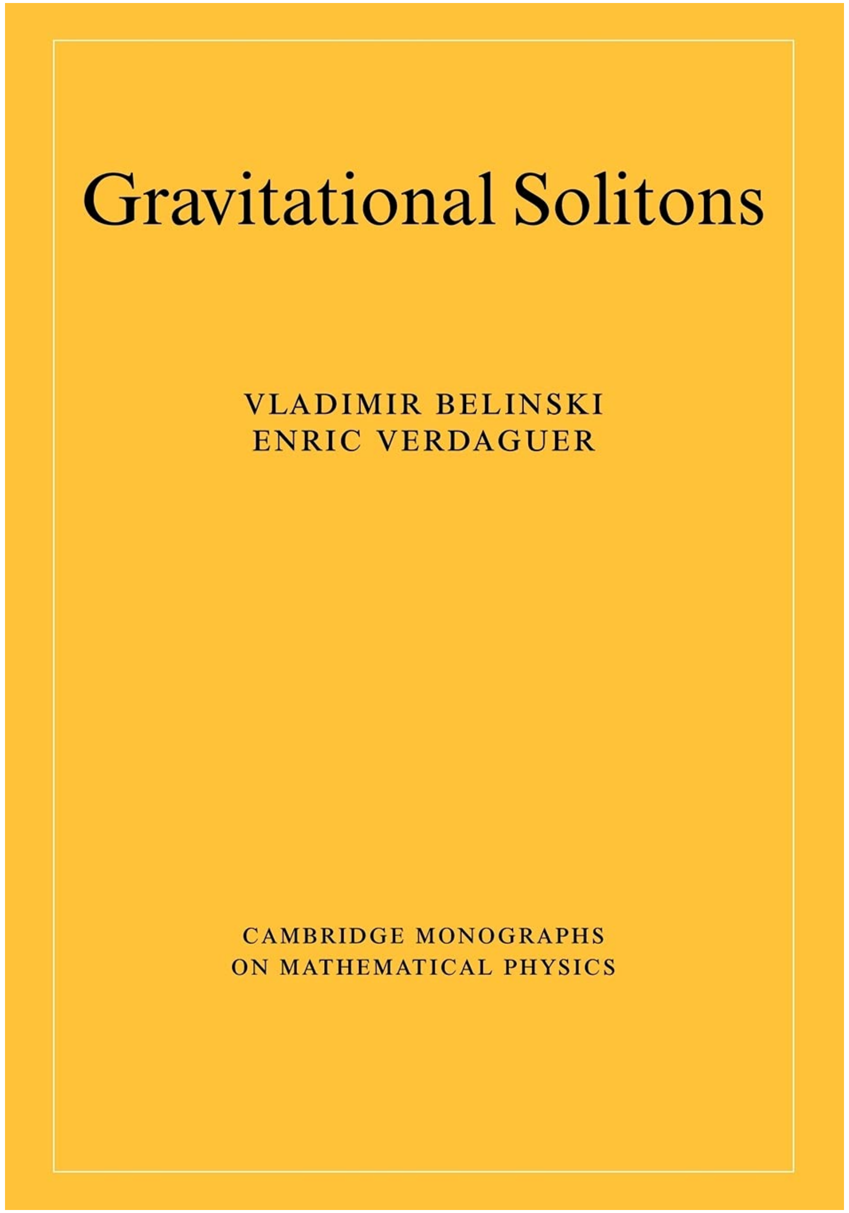

V Belinski
E Verdaguer

Cambridge UP 2001

$$ds^2 = f^{-1}[e^{2\gamma}(d\rho^2 + dz^2) + \rho^2 d\varphi^2] - f(dt - \omega d\varphi)^2 \tag{2.1}$$

Here ρ, φ, z and t are canonical Weyl coordinates and time, respectively; $f(\rho, z)$, $\gamma(\rho, z)$ and $\omega(\rho, z)$ are unknown functions to be determined from the field equations.

The vacuum Einstein equations are given by

$$R_{ik} = 0,$$

where R_{ik} is the Ricci tensor .

Therefore we obtain all the Einstein equations in the case of a stationary axially symmetric gravitational field outside the sources:

$$f\Delta f = (\vec{\nabla} f)^2 - f^4\rho^{-2}(\vec{\nabla}\omega)^2, \tag{2.2}$$

$$\vec{\nabla}(f^2\rho^{-2}\vec{\nabla}\omega) = 0, \tag{2.3}$$

$$\frac{\partial\gamma}{\partial\rho} = \frac{1}{4}\rho f^{-2}[(\frac{\partial f}{\partial\rho})^2 - (\frac{\partial f}{\partial z})^2 - f^4\rho^{-2}((\frac{\partial\omega}{\partial\rho})^2 - (\frac{\partial\omega}{\partial z})^2)], \tag{2.4}$$

$$\frac{\partial\gamma}{\partial z} = \frac{1}{2}\rho f^{-2}(\frac{\partial f}{\partial\rho}\frac{\partial f}{\partial z} - f^4\rho^{-2}\frac{\partial\omega}{\partial\rho}\frac{\partial\omega}{\partial z}), \tag{2.5}$$

The operators $\vec{\nabla}$ and Δ defined by the formulae

$$\vec{\nabla} \equiv \vec{\rho}_0\frac{\partial}{\partial\rho} + \vec{z}_0\frac{\partial}{\partial z}$$

$$\Delta \equiv \vec{\nabla}^2 \equiv \frac{\partial^2}{\partial\rho^2} + \frac{1}{\rho}\frac{\partial}{\partial\rho} + \frac{\partial^2}{\partial z^2},$$

1. If we switch from the rotation potential ω to the new potential Φ by the formulae

$$\frac{\partial\omega}{\partial\rho} = \frac{\rho}{f^2}\frac{\partial\Phi}{\partial z}, \quad \frac{\partial\omega}{\partial z} = -\frac{\rho}{f^2}\frac{\partial\Phi}{\partial\rho}, \tag{2.13}$$

or, in the prolate ellipsoidal coordinates,

$$\frac{\partial\omega}{\partial x} = \frac{k_0(1-y^2)}{f^2}\frac{\partial\Phi}{\partial y}, \quad \frac{\partial\omega}{\partial y} = -\frac{k_0(x^2-1)}{f^2}\frac{\partial\Phi}{\partial x}, \tag{2.14}$$

we obtain the following field equations:

$$f\Delta f = (\vec{\nabla} f)^2 - (\vec{\nabla}\Phi)^2, \quad \vec{\nabla}(f^{-2}\vec{\nabla}\Phi) = 0. \tag{2.15}$$

$$f^{-1}\overrightarrow{\nabla} f = \overrightarrow{A}, \quad f^{-1}\overrightarrow{\nabla}\Phi = \overrightarrow{B}. \tag{2.16}$$

In this case, from we obtain the following set of four first-order differential equations for $\overrightarrow{A}$ and $\overrightarrow{B}$:

$$div\overrightarrow{A} = -\overrightarrow{B}^2, \quad div\overrightarrow{B} = (\overrightarrow{A}\cdot\overrightarrow{B}),$$

$$rot\overrightarrow{A} = 0, \quad rot\overrightarrow{B} = -[\overrightarrow{A}\times\overrightarrow{B}], \tag{2.17}$$

This form of the field equations was developed in [28], [29]. In the Weyl canonical coordinates we can rewrite 2.16 as

$$A_1 = \frac{1}{f}\frac{\partial f}{\partial\rho}, \quad A_2 = \frac{1}{f}\frac{\partial f}{\partial z},$$

$$B_1 = \frac{1}{f}\frac{\partial\Phi}{\partial\rho}, \quad B_2 = \frac{1}{f}\frac{\partial\Phi}{\partial z}, \tag{2.18}$$

In this case, using 2.17 and 2.18, we obtain

$$\frac{1}{\rho}\frac{\partial}{\partial\rho}(\rho A_1) + \frac{\partial A_2}{\partial z} = -(B_1^2 + B_2^2),$$

$$\frac{1}{\rho}\frac{\partial}{\partial\rho}(\rho B_1) + \frac{\partial B_2}{\partial z} = A_1B_1 + A_2B_2, \tag{2.19}$$

$$\frac{A_1}{\partial z} - \frac{A_2}{\partial\rho} = 0, \quad \frac{B_1}{\partial z} - \frac{B_2}{\partial\rho} = A_2B_1 - A_1B_2.$$

Introducing the Ernst complex potential

$$\varepsilon = f + i\Phi \tag{2.22}$$

gives us, from 2.15, the equation

$$(\varepsilon + \varepsilon^*)\Delta\varepsilon = 2(\vec{\nabla}\varepsilon)^2, \tag{2.23}$$

where ε^* is the complex conjugate of ε.
A transformation of 2.23

$$\varepsilon = (\xi - 1)(\xi + 1)^{-1}, \tag{2.24}$$

leads to one more form of the equations for a stationary axially symmetric gravitational field:

$$(\xi\xi^* - 1)\Delta\xi = 2\xi^*(\vec{\nabla}\xi)^2. \tag{2.25}$$

For Equation 2.23 we can prove the following theorem :
Theorem 1. *If* $\tilde{\varepsilon}$ *is a solution of equation, then the functions*

$$\varepsilon = \frac{iA_0 + B_0\tilde{\varepsilon}}{C_0 + iD_0\tilde{\varepsilon}}, \quad \varepsilon^* = \frac{-iA_0 + B_0\tilde{\varepsilon}^*}{C_0 - iD_0\tilde{\varepsilon}^*}, \tag{2.26}$$

where A_0, B_0, C_0 *and* D_0 *are arbitrary real constants subject to the constraint* $A_0D_0 + B_0C_0 \neq 0$, *also satisfy Equation 2.23.*
Its proof can be obtained immediately by substitution of into the corresponding Equation in 2.23.

2. The substitution $f = \rho/F$ in equations gives us the following equations:

$$F\Delta F = (\vec{\nabla} F)^2 + (\vec{\nabla}\omega)^2, \quad \vec{\nabla}(F^{-2}\vec{\nabla}\omega) = 0. \tag{2.33}$$

The set of two second-order differential equations can also be reduced to a set of four first-order differential equations.

If we introduce the notations

$$F^{-1}\vec{\nabla} F = A, \quad F^{-1}\vec{\nabla}\omega = B, \tag{2.34}$$

we obtain (2.17).

Introducing the functions

$$\varepsilon_1 = F + \omega \quad \varepsilon_2 = F - \omega, \tag{2.35}$$

we rewrite Equations (2.33) in the symmetric form

$$(\varepsilon_1 + \varepsilon_2)\Delta\varepsilon_1 = 2(\vec{\nabla}\varepsilon_1)^2,$$
$$(\varepsilon_1 + \varepsilon_2)\Delta\varepsilon_2 = 2(\vec{\nabla}\varepsilon_2)^2. \tag{2.36}$$

For the field equations and one can prove theorems, similar to and. So, for equations we have the following theorem.

Theorem 2. *If $\tilde{\varepsilon}_1$ and $\tilde{\varepsilon}_2$ are solution of equations , then the functions*

The four types of solutions representing the exterior gravitational fields of bound masses are classified as follows:

$$
\begin{array}{ccc}
\text{Schwarzshild metric} & \xrightarrow{\text{rotation}} & \text{Kerr metric} \\
(\rho\neq0,\ \omega=\sigma=0) & & (\rho\neq0,\ \omega\neq0,\ \sigma=0) \\
\Big\downarrow \text{deformation} & & \Big\downarrow \text{deformation} \\
\text{Weyl metric} & \xrightarrow{\text{rotation}} & \text{T-S metrics} \\
(\rho\neq0,\ \omega=0,\ \sigma\neq0) & & (\rho\neq0,\ \omega\neq0,\ \sigma\neq0).
\end{array}
$$

In the above diagram, ρ, ω and σ denote divergence, rotation and shear of bunch of null geodesics in the corresponding space-times.[8] As seen from the above

In the cases of no rotation, many solutions for ξ are easily obtainable, which derive the Weyl metrics. In these solutions there exists an interesting series of solutions[11),12)] with a positive parameter δ, expressed in the form

$$\xi=\frac{(x+1)^{\delta}+(x-1)^{\delta}}{(x+1)^{\delta}-(x-1)^{\delta}}, \tag{2·8}$$

where prolate spheroidal coordinates (x, y) are used in place of cylindrical coordinates (ρ, z), and the two coordinates are related as follows,

$$\rho=\kappa(x^2-1)^{1/2}(1-y^2)^{1/2}, \quad z=\kappa xy\,. \tag{2·9}$$

The metrics obtained from the solutions (2·8) are regarded as representing the gravitational fields of axi-symmetric masses, whose deformation is described by δ. In particular, in the case $\delta=1$ the Schwarzshild metric is obtained and it

$$\xi = \frac{\alpha}{\beta}, \tag{2·10}$$

where α and β are complex polynomials of x and y. Substituting Eq. (2·10) into Eq. (2·2) and using the coordinates (x, y), we obtain the basic equation as

$$\Big[(x^2-1)(\alpha\alpha^* - \beta\beta^*)\Big(\frac{\partial^2 \alpha}{\partial x^2}\beta - \alpha\frac{\partial^2 \beta}{\partial x^2}\Big) + \Big\{2x(\alpha\alpha^* - \beta\beta^*) - 2(x^2-1)$$
$$\times\Big(\alpha^*\frac{\partial \alpha}{\partial x} - \beta^*\frac{\partial \beta}{\partial x}\Big)\Big\}\Big(\frac{\partial \alpha}{\partial x}\beta - \alpha\frac{\partial \beta}{\partial x}\Big)\Big]$$
$$-[\text{the same expression replacing } x \text{ by } y] = 0 . \tag{2·11}$$

The solutions which have been obtained are as follows:

i) *Ernst's solution*[10] *or the T-S solution for* $\delta = 1$

$$\alpha = px - iqy \quad \text{and} \quad \beta = 1 , \tag{2·12}$$

where p and q are parameters relating to each other as $p^2 + q^2 = 1$. In the case of no rotation, $p = 1$ and $q = 0$. This solution gives the well-known Kerr metric.

ii) *the T-S solution for* $\delta = 2$[3]

$$\alpha = p^2x^4 + q^2y^4 - 1 - 2ipqxy(x^2 - y^2)$$

and

$$\beta = 2px(x^2-1) - 2iqy(1-y^2). \tag{2·13}$$

「当て嵌め」ーー＞ソリトン数学

非線形重力波　重力ソリトン
Einstein-Maxwell

Lie symmetries

Prolongation

Linearized equation

Backlund transformation

Belenski-Zakharov technique

Rieman-Hilbert problem

Harmonic maps

Variational Backlund transformations

Hirota’s method

群論的
Kinnersley-Chitre

逆散乱法

ベックルンド法

Ernst方程式の
Omote-Wadachi　1981
PTP65,1621
JMP 22,961

Double-Kerr

The Ernst potential ξ of the solution obtained by Kramer and Neugebauer is

$$\xi=\frac{\begin{vmatrix} S_1 & S_2 & S_3 & S_4 \\ 1 & 1 & 1 & 1 \\ K_1 & K_2 & K_3 & K_4 \\ K_1{}^2 & K_2{}^2 & K_3{}^2 & K_4{}^2 \end{vmatrix}}{\begin{vmatrix} S_1 & S_2 & S_3 & S_4 \\ 1 & 1 & 1 & 1 \\ K_1 & K_2 & K_3 & K_4 \\ K_1S_1 & K_2S_2 & K_3S_3 & K_4S_4 \end{vmatrix}}, \qquad (2\cdot1)$$

where

$$S_m=e^{i\omega_m}r_m\,, \qquad r_m=[\rho^2+(z-K_m)^2]^{1/2}, \qquad (2\cdot2)$$

ω_m and K_m are real parameters and $m=1, \cdots, 4$.[5] Equation (2·1) is written also

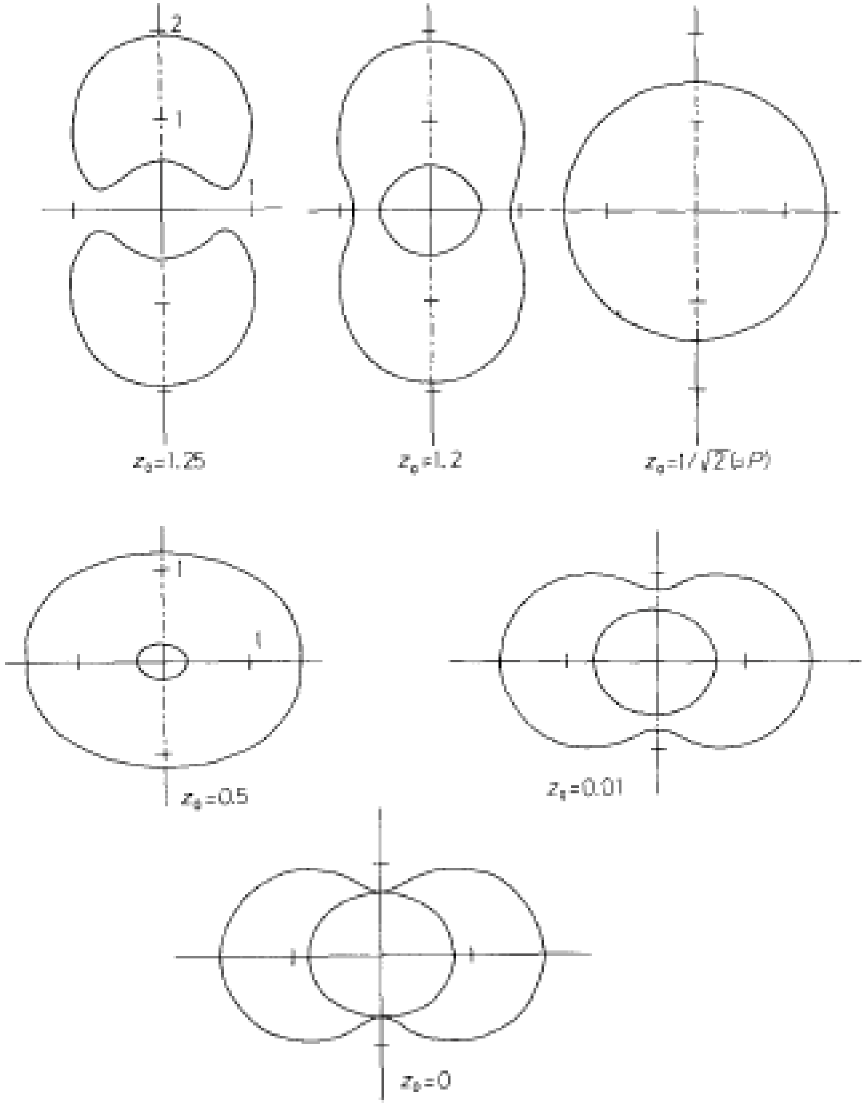

Fig. 2. The contours of the infinite redshift surface of the same metric with Fig. 1(i), i. e., parallel case, except different values of z_0 like 1.25, 1.2, $1/\sqrt{2}$, 0.5, 0.1 and 0. The $z_0=1/\sqrt{2}$ and $z_0=0$ cases correspond to the one Kerr metric and the Tomimatsu-Sato $\delta=2$ metric respectively.

The K-C solution is a vacuum specialization of the nine-parameter electrovac rational function solution considered in the paper[30] and, therefore, its metric functions f, γ, ω are defined by the following expressions:*)

$$f = \frac{E_+\bar{E}_- + \bar{E}_+E_-}{2E_-\bar{E}_-}, \qquad e^{2\gamma} = \frac{E_+\bar{E}_- + \bar{E}_+E_-}{2K_0\bar{K}_0 r_1^4 r_2^4}, \qquad \omega = -\frac{4\mathrm{Im}(\bar{E}_- G)}{E_+\bar{E}_- + \bar{E}_+E_-}, \tag{A·1}$$

where $r_i = \sqrt{\rho^2 + (z-\alpha_i)^2}$, the determinants $E_\pm$ and G have the form

$$E_\pm = \begin{vmatrix} 1 & 1 & 1 & (z-\alpha_1)/r_1 & (z-\alpha_2)/r_2 \\ \pm 1 & & & & \\ \pm 1 & & & & \\ 0 & & \mathcal{M} & & \\ 0 & & & & \end{vmatrix},$$

$$G = \begin{vmatrix} 0 & r_1+\alpha_1-z & r_2+\alpha_2-z & \rho^2/r_1 & \rho^2/r_2 \\ -1 & & & & \\ -1 & & & & \\ 0 & & \mathcal{M} & & \\ 0 & & & & \end{vmatrix},$$

$$\mathcal{M} = \begin{pmatrix} \dfrac{r_1}{\alpha_1-\beta_1} & \dfrac{r_2}{\alpha_2-\beta_1} & -\dfrac{r_1^2}{(\alpha_1-\beta_1)^2} & -\dfrac{r_2^2}{(\alpha_2-\beta_1)^2} \\ \dfrac{r_1}{\alpha_1-\beta_2} & \dfrac{r_2}{\alpha_2-\beta_2} & -\dfrac{r_1^2}{(\alpha_1-\beta_2)^2} & -\dfrac{r_2^2}{(\alpha_2-\beta_2)^2} \\ \dfrac{1}{\alpha_1-\bar{\beta}_1} & \dfrac{1}{\alpha_2-\bar{\beta}_1} & r_1^2\dfrac{\partial}{\partial\alpha_1}\left[\dfrac{1}{(\alpha_1-\bar{\beta}_1)r_1}\right] & r_2^2\dfrac{\partial}{\partial\alpha_2}\left[\dfrac{1}{(\alpha_2-\bar{\beta}_1)r_2}\right] \\ \dfrac{1}{\alpha_1-\bar{\beta}_2} & \dfrac{1}{\alpha_2-\bar{\beta}_2} & r_1^2\dfrac{\partial}{\partial\alpha_1}\left[\dfrac{1}{(\alpha_1-\bar{\beta}_2)r_1}\right] & r_2^2\dfrac{\partial}{\partial\alpha_2}\left[\dfrac{1}{(\alpha_2-\bar{\beta}_2)r_2}\right] \end{pmatrix}, \tag{A·2}$$

and the determinant K_0 is defined by the 4×4 matrix obtainable from $\mathcal{M}$ by simply setting r_1 and r_2 to unity.

In this paper, we focus on the $\delta = 2$ Tomimatsu-Sato metric. The properties of the corresponding spacetime that have been found so far are summarized as follows [6, 7].

Ring singularity: This spacetime has a ring singularity at the root of $B(x, y = 0) = 0$. (The cross in Figure 1)

Ergosphere: The timelike Killing vector becomes null at the roots of A. There are two single roots for $x \geq 1$ (The dotted lines in Figure 1), the smaller of which coincides with the ring singularity.

Causality violation region: Since ϕ is the periodic angular coordinate, this spacetime has closed timelike loops in the region with negative $g_{\phi\phi}$. (The shaded portion in Figure 1)

Directional singularity: This metric has directional singularities at the points $(\rho, z) = (0, \pm\sigma)$, where the value of a curvature invariant has different limits when the point is approached from different directions. (The two filled circles in Figure 1)

The nature of the surface $x = 1$: In the Kerr case, $x = 1(\rho = 0, |z| \leq \sigma)$ surface is an event horizon. However, in the $\delta = 2$ Tomimatsu-Sato case, this is not the case. Because the induced metric is Lorentzian and two Killing vectors ∂_t and ∂_ϕ become parallel there, $x = 1$ surface cannot be a null surface.

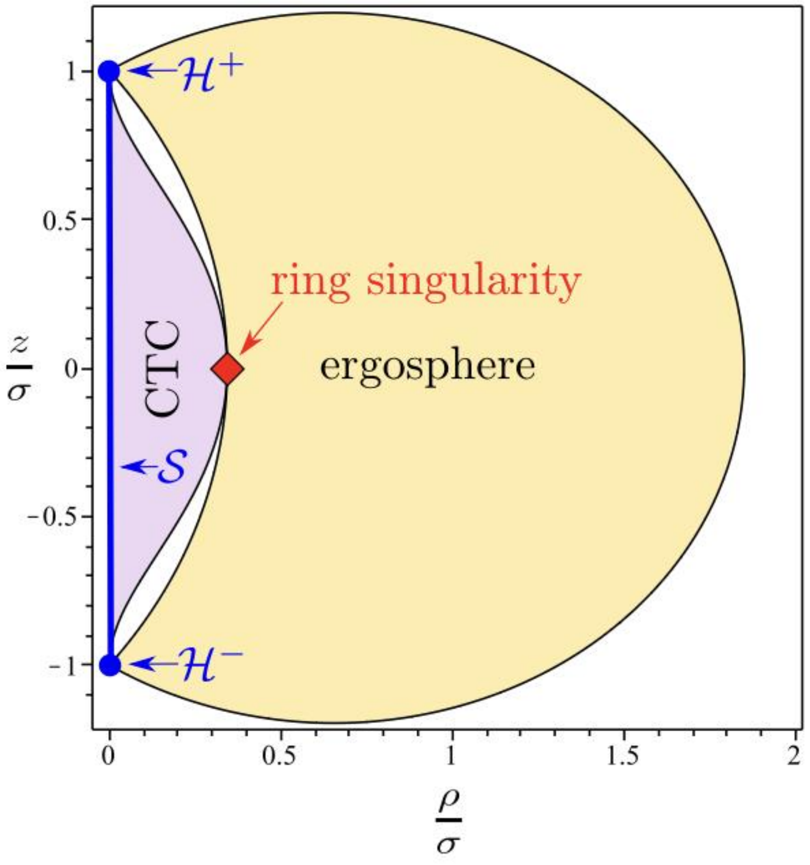

Figure 2: The ergosphere (tan) and the region with closed timelike curves (CTCs) (purple) when $p = 0.8$. The boundaries of the ergoshere are lines $\theta =$ constant.

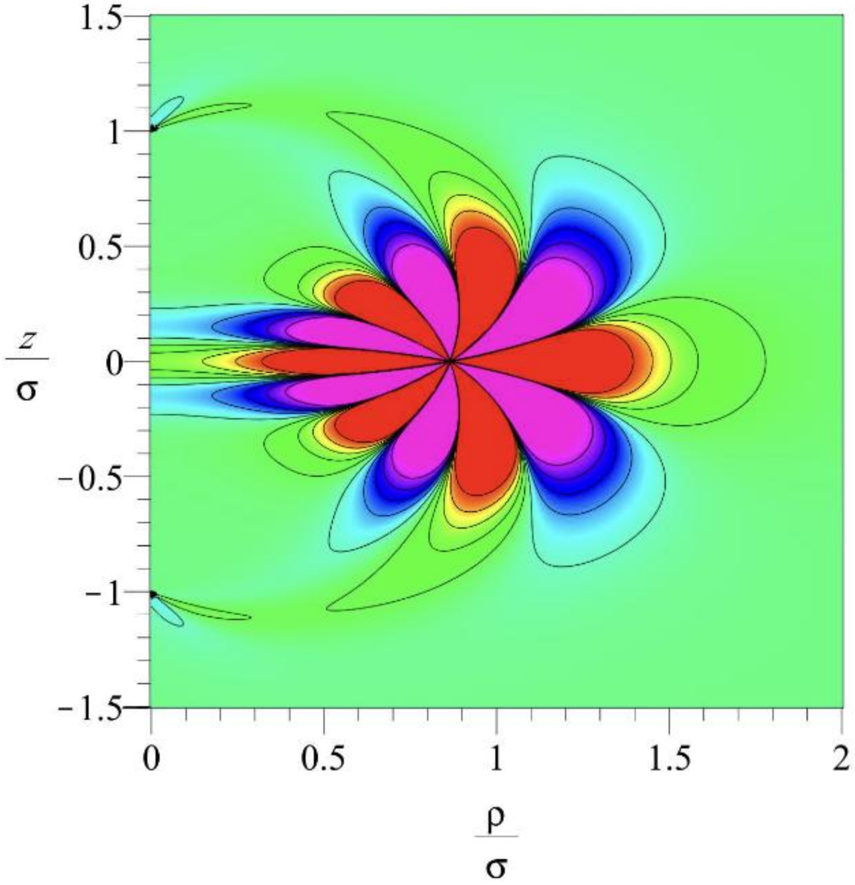

Figure 3: Contour plot of the Kretchmann scalar $\tanh(\sigma^{-4}R_{\alpha\beta\gamma\delta}R^{\alpha\beta\gamma\delta})$ in the (ρ, z) plane for $p = 1/3$. The centre of the flower-shaped region is the ring singularity.

Kodama-Hikida 2003

Two poles

Two degenerate Killing horizons

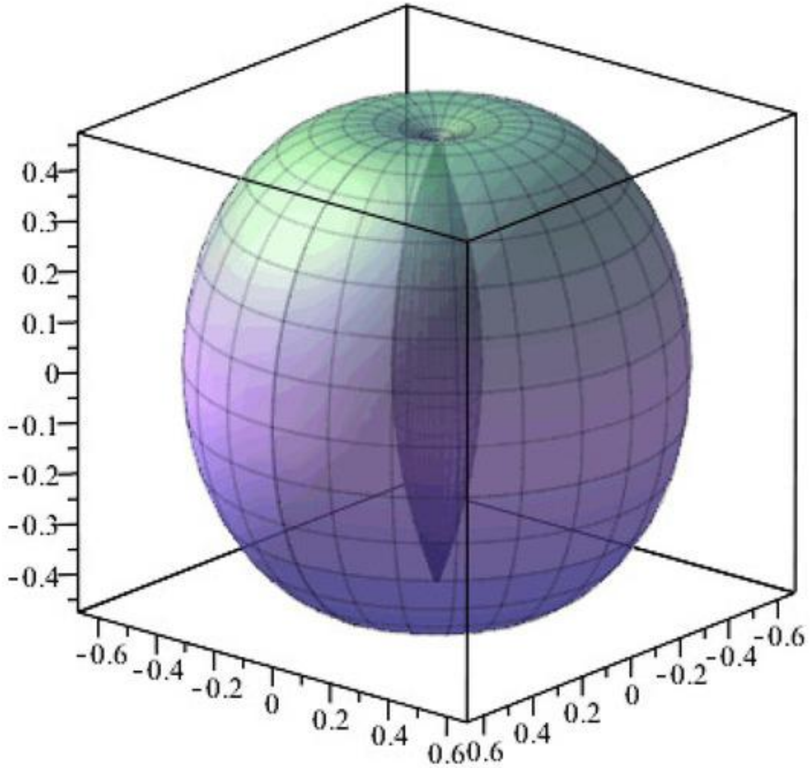

We have investigated the structure of the $\delta = 2$ Tomimatsu-Sato spacetime. By introducing an appropriate coordinate system, we have shown that the two points in the Weyl coordinates, which have been recognized as the directional singularities, are really two-dimensional surfaces and that these surfaces are horizons. We have also shown that each of the two horizons has the topology of a sphere. This result is rather surprising because the $\delta = 2$ Tomimatsu-Sato solution is obtained from the Neugebauer-Kramer solution representing a superposition of two Kerr solutions, as the limit that the centers of two black holes coincide [9]. This may indicates a new possibility for the final states of gravitational collapse.

Manko 2012

Double-Kerr(NUT) vs TS2
Double、 同じ vs 違う Kerr,

negative Komar-mass

CTC 出現

負質量 Kerr CTC

Euclidon metric の重ね合わせでKerr

Stationary multiple euclidon solutions to the vacuum Einstein equations

Aleksandr A. Shaideman, Kirill V. Golubnichiy

http://arxiv.org/abs/2502.03675v1

$$f\Delta f = (\vec{\nabla} f)^2 - (\vec{\nabla}\Phi)^2, \quad f\Delta\Phi = 2\vec{\nabla}\Phi\vec{\nabla} f,$$

$$\frac{\partial\omega}{\partial\rho} = \frac{\rho}{f^2}\frac{\partial\Phi}{\partial z}, \quad \frac{\partial\omega}{\partial z} = -\frac{\rho}{f^2}\frac{\partial\Phi}{\partial\rho}. \tag{4.1}$$

$(f^0, \quad \Phi^0, \quad \omega^0)$ - we call the seed solution.

One of the simplest solutions of Equation (4.1) is the one-stationary euclidon solution

$$f_E = \frac{(z-z_1) + \sqrt{\rho^2 + (z-z_1)^2}\tanh U_0}{C_1},$$

$$\Phi_E = \frac{\sqrt{\rho^2 + (z-z_1)^2}}{C_1\cosh U_0} + C_2, \tag{4.2}$$

$$\omega_E = C_1\frac{\sqrt{\rho^2 + (z-z_1)^2}}{(z-z_1) + \sqrt{\rho^2 + (z-z_1)^2}\cdot\tanh U_0}\cdot\frac{1}{\cosh U_0} + C_3,$$

where U_0, C_1, C_2, and C_3 are arbitrary constants.

Straightforward calculations show the solution (4.2) turns all components of the Riemann-Christoffel curvature tensor to zero. Thus, it makes sense to call the solution (4.2) a euclidon solution. One can say that it characterizes some relativistic noninertial frame of reference in flat space-time. Nevertheless, the solution (4.2) allows one to generate solutions describing curved space-time.

$$
\begin{aligned}
\tilde{f} &= \frac{z - z_1 + R \tanh U}{f_0}, \\
\tilde{\Phi} &= \frac{R}{f_0 \cosh U} + \omega_0, \\
\tilde{\omega} &= \frac{f_0 (z - z_1) \coth U}{(z - z_1) \cosh U + R \sinh U} + \Phi_0 .
\end{aligned}
$$

Only U remains to be determined.

$$f_0 = f_0(r,z), \qquad \Phi_0 = 0, \qquad \omega_0 = 0.$$

$$f_0 = \mathrm{e}^{\chi}, \tag{18}$$

the Einstein equations (4), (5) reduce to

$$\Delta\chi = 0. \tag{19}$$

For such an harmonic function χ, the solution (17) is said to be Lewis-type [3]. Hence, the system (9) in [1] permitting one to determine the U function reduces to

$$U_{,r} = a_1\chi_{,r} + a_2\chi_{,z}, \tag{20}$$

$$U_{,z} = -a_2\chi_{,r} + a_1\chi_{,z}, \tag{21}$$

where

$$a_1 = \frac{z - z_1}{R}, \qquad a_2 = \frac{r}{R}, \qquad a_1^2 + a_2^2 = 1. \tag{22}$$

$$\chi = \ln[z_1(\lambda + 1)(\mu + 1)], \tag{29}$$

where χ obeys (19).

The system (20)-(21), determining the potential $U(\lambda, \mu)$, now takes the form

$$U_{,\lambda} = \frac{\lambda\mu - 1}{\lambda - \mu}\chi_{,\lambda} + \frac{1 - \mu^2}{\lambda - \mu}\chi_{,\mu}, \tag{30}$$

$$U_{,\mu} = -\frac{\lambda^2 - 1}{\lambda - \mu}\chi_{,\lambda} + \frac{\lambda\mu - 1}{\lambda - \mu}\chi_{,\mu}. \tag{31}$$

Hence, we find by integration

$$U = \ln\left[\frac{1+\lambda}{a_0(1+\mu)}\right], \tag{32}$$

where a_0 is a constant. On the other hand, (23) becomes, in prolate spheroidal coordinates,

$$\begin{aligned}(\lambda-\mu)[(\lambda^2-1)U_{,\lambda\lambda}+(1-\mu^2)U_{,\mu\mu}]\\ -2(\lambda\mu-1)(U_{,\lambda}+U_{,\mu})=0,\end{aligned} \tag{33}$$

and it can be easily checked that (32) is a solution to (33). Eqs. (14)-(15), giving $\tilde{f}$ and $\tilde{\Phi}$, now become

$$\tilde{f}(\lambda,\mu) = \frac{\lambda\mu-1+(\lambda-\mu)\tanh U}{(\lambda+1)(\mu+1)}, \tag{34}$$

$$\tilde{\Phi}(\lambda,\mu) = \frac{\lambda-\mu}{(\lambda+1)(\mu+1)\cosh U} \tag{35}$$

膨張宇宙でのボイドの膨張

計量テンソルの張り合わせ

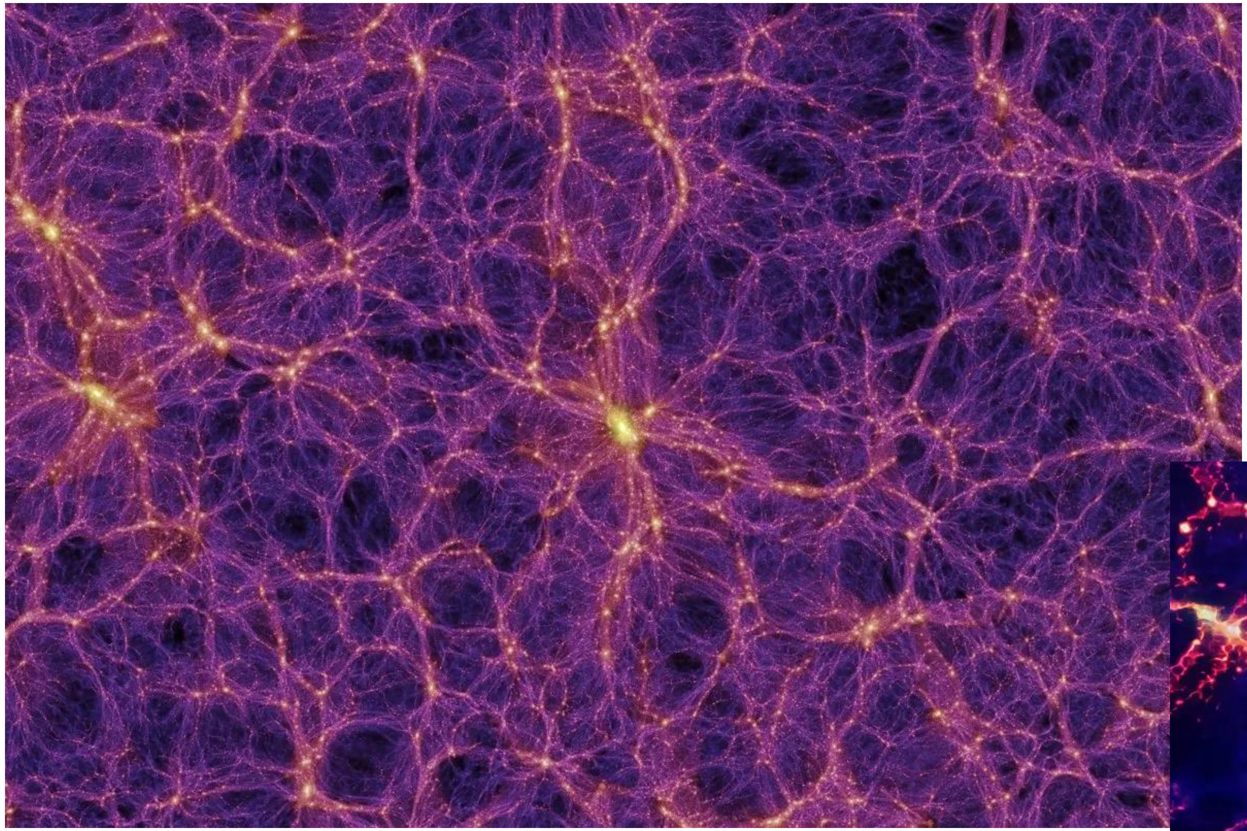

銀河分布の空洞Void

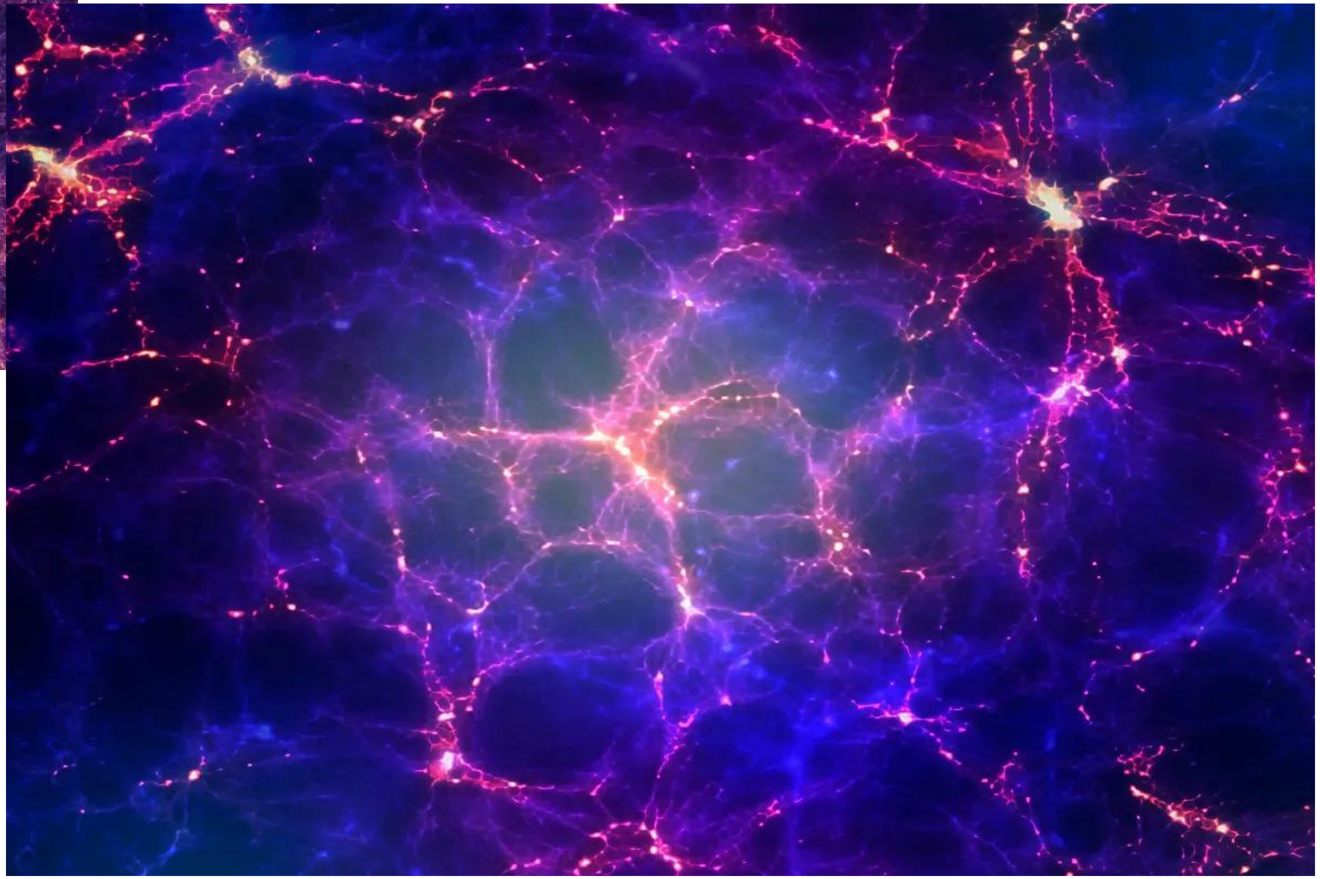

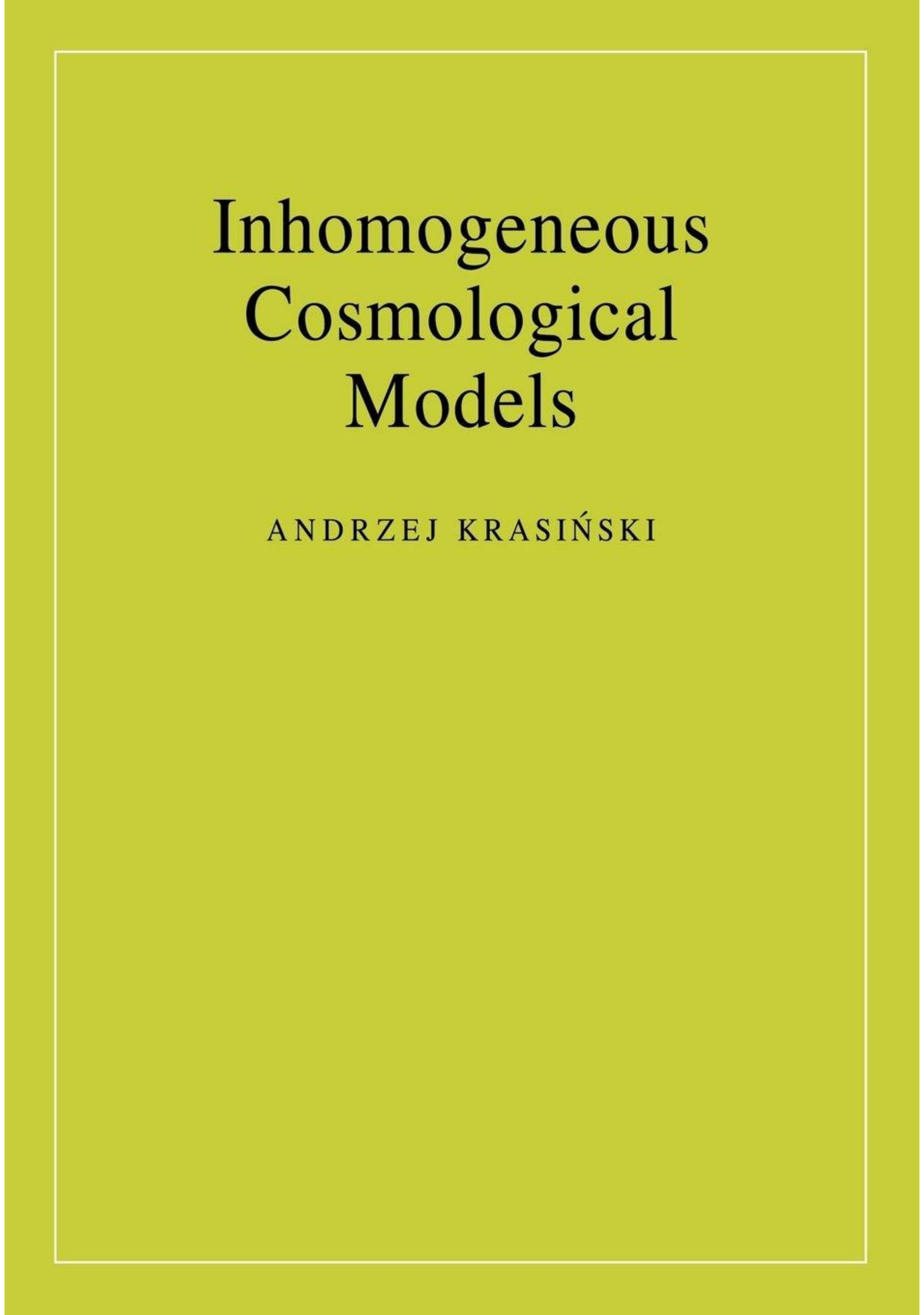

A Krasinski

Cambridge UP
1997

球対称

・Einstein-Strauss

・shell-crossng

計量の張り合わせ　Israel 方法

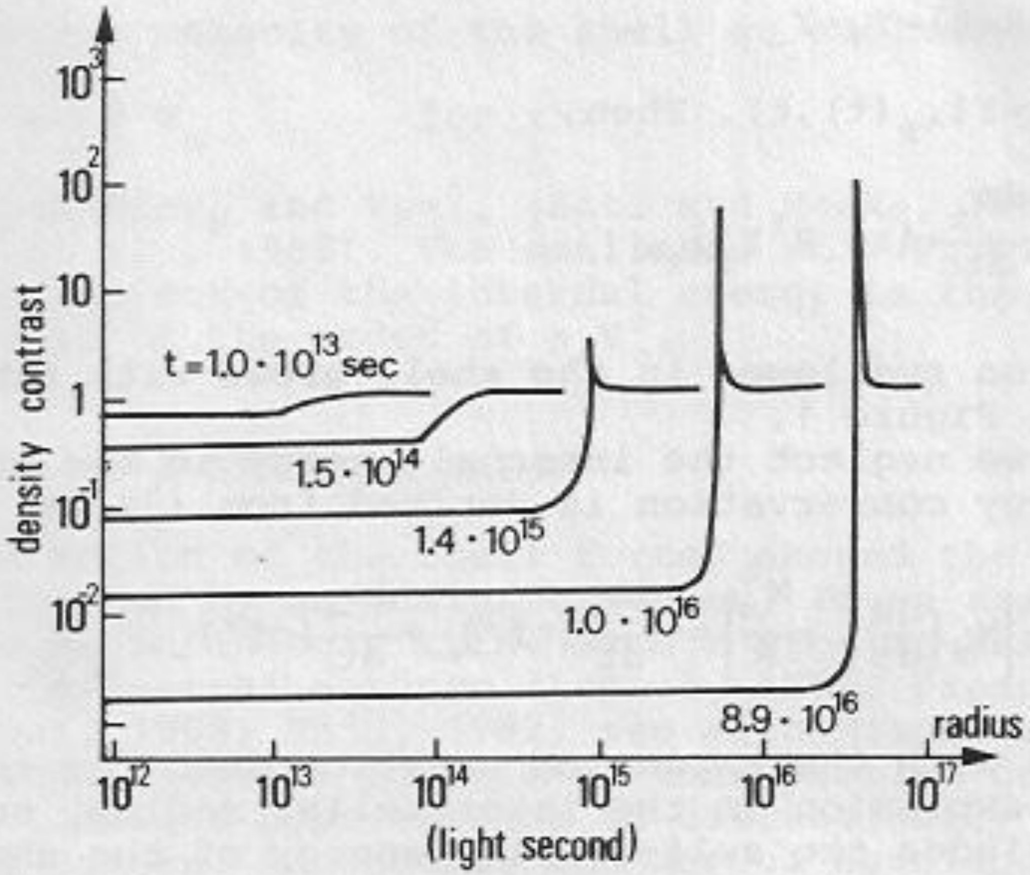

. As the negative density perturbation grows, the shock wave is generated surrounding this region and propagates outwards accumulating the expanding matter in the flat universe (Suto et al., 1984).

須藤　靖

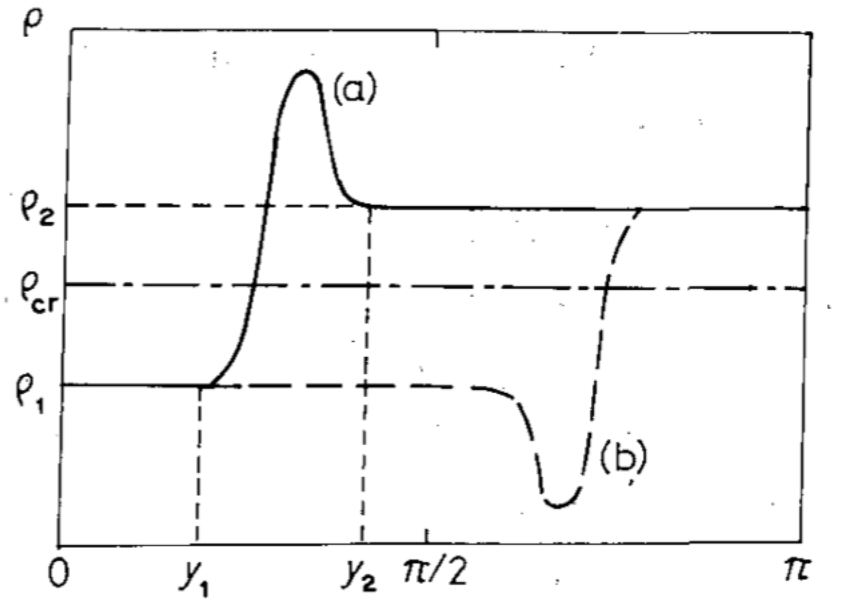

Fig. 1. A schematic density distribution $\rho(y)$ for (a) "a small void" and (b) "a large void".

$$\rho_i = \rho(t_i)(1-\delta), \qquad \chi \leq \chi_v$$

$$= \rho(t_i)\{1-\delta(\chi_v/\chi)^n\}, \qquad \chi > \chi_v$$

$$\rho_i = \rho(t_i)(1-\delta), \qquad \chi \le \chi_v$$
$$= \rho(t_i)\{1-\delta(\chi_v/\chi)^n\}, \qquad \chi > \chi_v$$

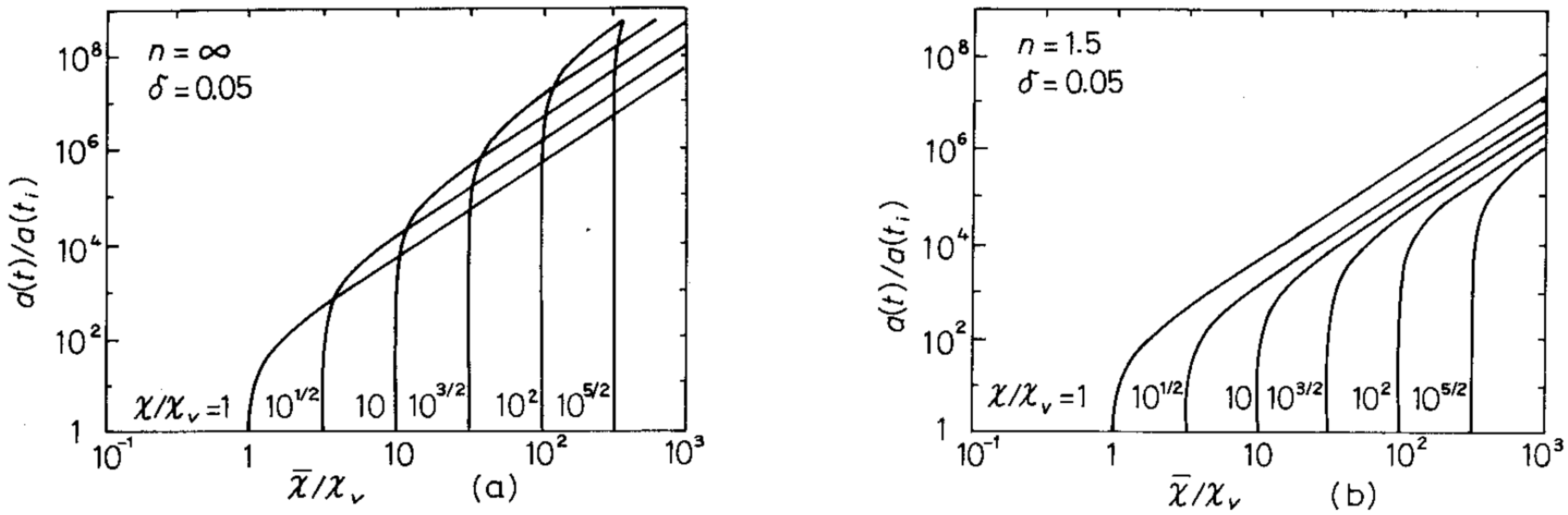

Fig. 1. The motion of the shells denoted by χ is shown using the coordinate χ defined by (3·1), for two cases of (a) $n=\infty$ and (b) $n=1.5$ taki[illegible] $n \ge 2$, the shell crossing occurs.

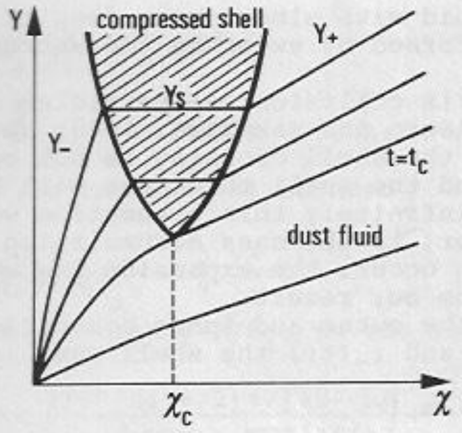

. A schematic diagram for the evolution of $Y(\chi,t)$. The shell-crossing starts to occur at t_c and χ_c where $Y'=0$. After that epoch, the mass in the hatched region has been compressed into a thin shell.

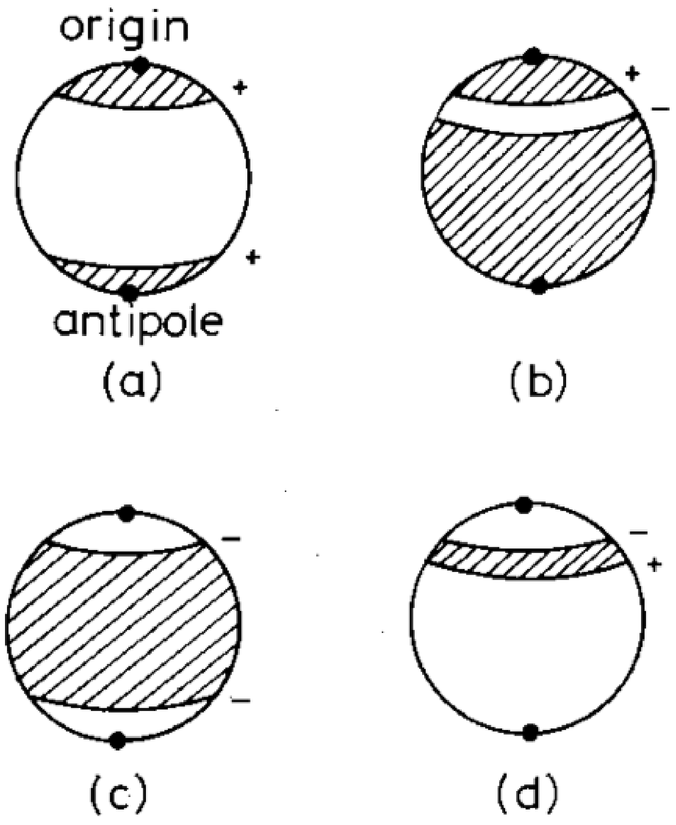

Fig. 2. Configuration of the perturbation with two shells. The region of void (less-dense region) is depicted by the hatch. The + and − denote the sign of $\delta\rho$ at the shell.

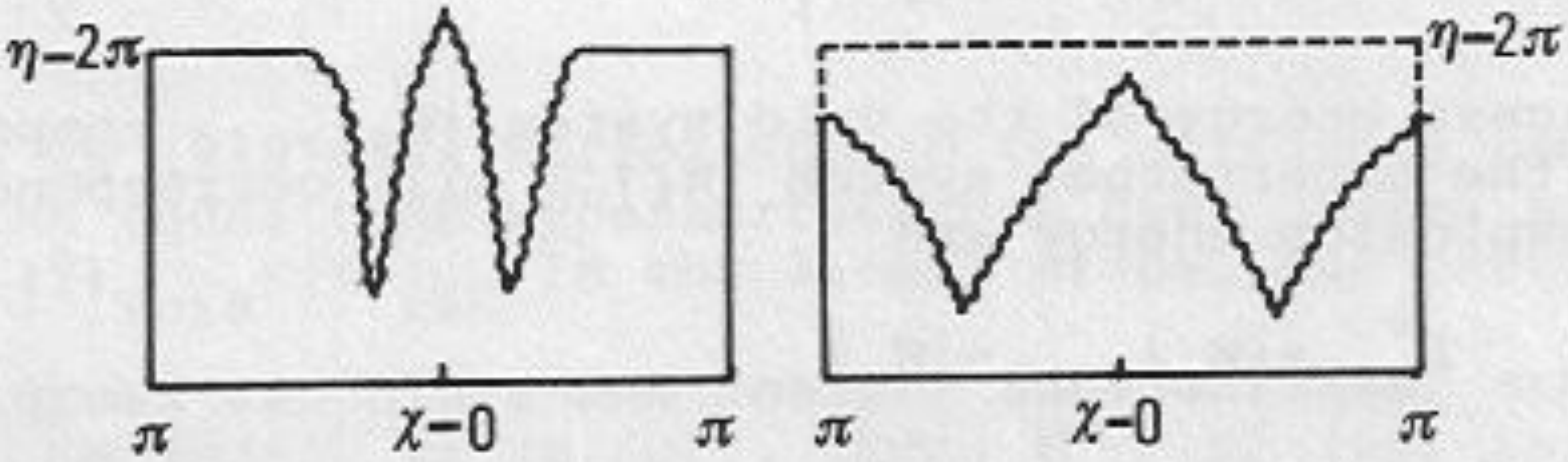

. 7. A schematic Penrose diagram of the closed universe with a void in it. If the void is large enough, the void occupies the whole space before the big crunch.

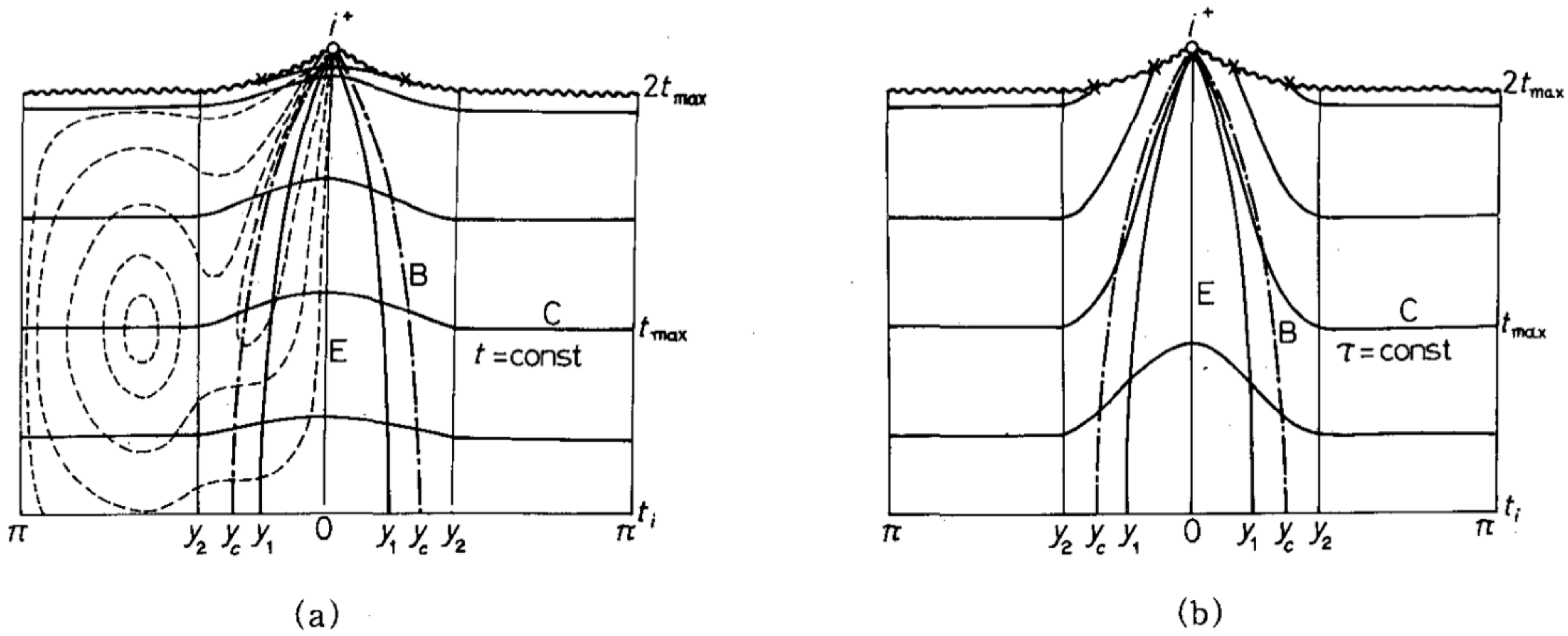

Fig. 3. Schematic diagram for global structure of the closed universe with one void. E and C denote "E-region" and "C-region" respectively and B is the boundary surface of $y=y_c$. In (a), the t=const hypersurfaces are depicted by solid lines and Y=const surfaces are shown by dotted lines, and in (b), the τ=const hypersurfaces are depicted. The future singularity is shown by a wavy line.

We introduce the Gauss coordinates in the neighbourhood of Σ in such a manner as

$$ds^2 = h_{ab} d\xi^a d\xi^b - dz^2 \tag{2·5}$$

with $z=0$ on Σ. Then, it is found that $\Gamma^z_{zz} = \Gamma^a_{zz} = \Gamma^z_{za} = 0$ on Σ. In this coordinate system, the Ricci tensor takes a form

$$R_{ab} = \frac{\partial \Gamma^z_{ab}}{\partial z} + (\Gamma^z_{ab}\Gamma^c_{zc} - 2\Gamma^c_{az}\Gamma^z_{cb} + {}^3R_{ab}) . \tag{2·6}$$

Substituting this relation into the Einstein equation $G_{\mu\nu} = -8\pi G T_{\mu\nu}$ and taking the integral over the Gauss coordinate through the infinitely thin shell, we get the relation

$$K^+_{ab} - K^-_{ab} = -8\pi G\left(S_{ab} - \frac{1}{2} h_{ab} S\right) \tag{2·7}$$

with

$$K^{\pm}_{ab} = \lim_{\Delta \to 0} \Gamma^z_{ab} = 2^{-1}(\partial h_{ab}/\partial z)_{\Sigma^{\pm}} \tag{2·8}$$

and

$$S_{ab} = \lim_{\Delta \to 0} \int_{-\Delta}^{\Delta} T_{ab} dz , \tag{2·9}$$

where we have used a boundedness of the bracket term in (2·6).

as $\boldsymbol{n}$, the hypersurface Σ is called "timelike" if $\boldsymbol{n}\cdot\boldsymbol{n}<0$ and "spacelike" if $\boldsymbol{n}\cdot\boldsymbol{n}>0$. In the conventional (1+3)ADM formalism, the hypersurface is taken to be spacelike. In the present problem, however, we consider a timelike hypersurface and the metric on Σ can be introduced as

$$dl^2=h_{ab}d\xi^a d\xi^b\ . \tag{2·2}$$

Using the Gauss-Codazzi relation, the Einstein tensor $G_{\mu\nu}$ is written in terms of extrinsic curvature K_{ab} and intrinsic curvature ${}^3R$ on Σ as

$$2G_{\mu\nu}n^\mu n^\nu={}^3R-K_{ab}K^{ab}+K^2 \tag{2·3}$$

and

$$G_{\mu\nu}\tilde{h}_a{}^\mu n^\nu=K^b_{a|b}-K_{|a}\ , \tag{2·4}$$

where $K_{ab}=\tilde{h}_a{}^\mu\tilde{h}_b{}^\nu n_{\mu;\nu}$, $\tilde{h}_a{}^\mu=\partial x^\mu/\partial\xi^a$ on Σ and $|$ denotes the covariant derivative in the space (2·2).

Spherically symmetric spacetime is written as

$$ds^2 = e^{\nu} dt^2 - e^{\lambda} dr^2 - r^2 d\Omega^2 \tag{A·1}$$

with $\nu(r, t)$, $\lambda(r, t)$ and $d\Omega^2 = d\theta^2 + \sin^2\theta d\varphi^2$. The metric of the hypersurface Σ, which is an evolutionary locus of the spherical shell, is written as

$$dl^2 = d\tau^2 - \rho(\tau)^2 d\Omega^2 \,, \tag{A·2}$$

where τ is the proper time of the shell and $4\pi\rho^2$ is a surface area. Due to the spherical symmetry, $S_2{}^2 = S_3{}^3$ and $K_2{}^2 = K_3{}^3$, where we take as $a = 0, 2, 3$ for τ, θ, φ, respectively.

For the metric form of (A·1), the extrinsic curvature is computed as[5)]

$$K_0{}^0 = -\sigma\left[\frac{\ddot{\rho} + \dot{\rho}^2(\lambda_{,r} + \nu_{,r})/2 + \nu_{,r} e^{-\lambda}/2}{\sqrt{\dot{\rho}^2 + e^{-\lambda}}} + \lambda_{,t}\dot{\rho} e^{(\lambda-\nu)/2}\right] \tag{A·3}$$

and

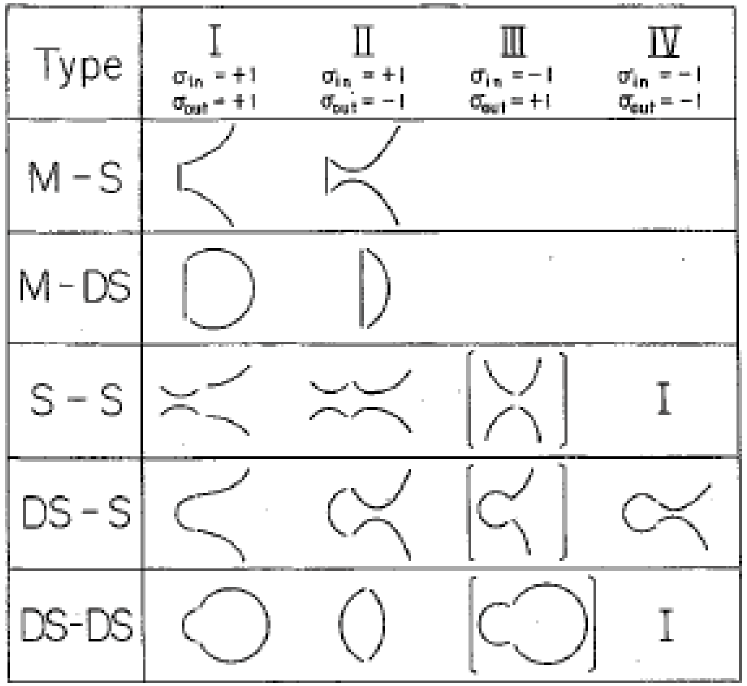

Fig. 1. Metric junctions among the Minkowski metric (M), the Schwarzschild metric (S) and the de Sitter metric (DS). The inner space where the center of spherical symmetry exists is written in the left like M("inner")-S("outer"). For each junction between the metrics, further differences specified by σ_{in} and σ_{out} are classified into types I ~IV. For each case, schematic pictures of the metric junction are given, where the "inner" space is written in the left.

The positive energy condition of the shell, (3·1), excludes some junctions like M-M, S-M and DS-M, those are not shown here. The type III cases drawn in the bracket [ ] are also excluded by the condition (3·1).

If we write the metric of M as

$$ds^2 = dT^2 - dR^2 - R^2 d\Omega^2 , \tag{4·6}$$

the proper time τ in (A·2) relates to T as $d\tau^2 = \{1-(dR/dT)^2\} dT^2$ and $(dR/dT) = (d\tau/dT)\dot{\rho} = \dot{\rho}/\sqrt{\dot{\rho}^2+1}$. Thus, the relation (4·5) is rewritten also

$$m_s\left(\frac{1}{\sqrt{1-(dR/dT)^2}} - 1\right) - \frac{1}{2}\frac{Gm_s^2}{R} = -(m_s - m_g) .$$

The second term on the left-hand side is interpreted as a gravitational self-energy of the shell. If $m_s > m_g$, the maximum radius is obtained from (4·5) as

$$\rho_{\max} = \frac{Gm_s^2}{2(m_s - m_g)} . \tag{4·7}$$

It $m_s < m_g$, ρ can take any values.

Subtracting (4·2) from (4·5), we get

$$2\sigma_{\text{out}}\sqrt{\dot{\rho}^2 + 1 - r_g/\rho} = (2m_g/m_s - Gm_s/\rho) . \tag{4·8}$$

Then, $\sigma_{\text{out}} \gtrless 0$ for $2m_g\rho \gtrless Gm_s^2$ respectively. Allowed region of motion on the ρ-(m_s/m_g) diagram is depicted in Fig. 2. As seen from this figure, the case of $m_g < m_s < 2m_g$ corresponds to the type I junction in Fig. 1 and the case of $m_s > 2m_g$ does to the type II junction. For $m_s = 2m_g$, $\rho_{\max} = r_g$ and the both cases coincides.

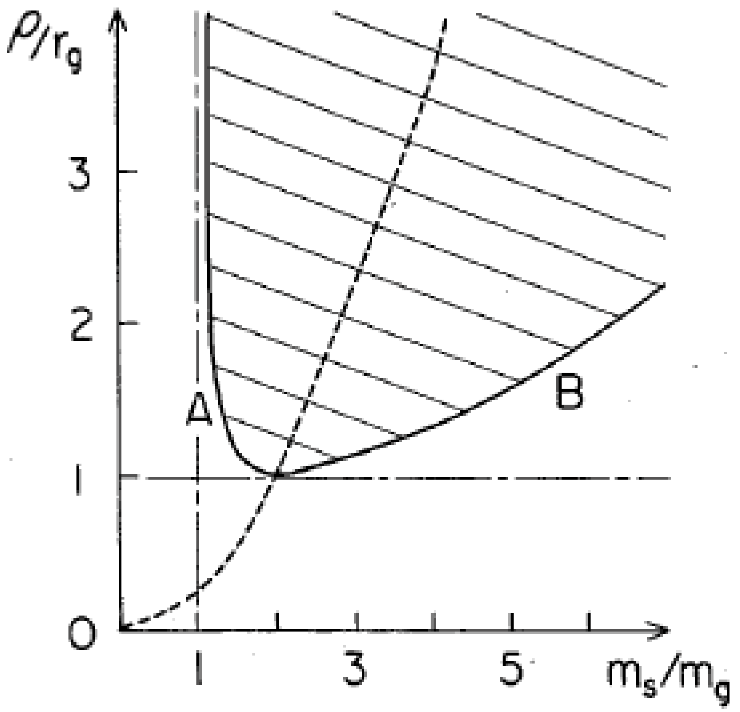

Fig. 2. For the dust shell at the Minkowski-Schwarzschild junction, allowed region of motion on the ρ-(m_s/m_g) diagram is given. The bold line shows ρ_{max} and the hatched region is a forbidden region of motion. The dotted line denotes $\rho/r_g=(m_s/m_g)^2/4$, which separates the sign of σ_{out}. The branch A is included in the type I junction and the B does in the type II. This figure as well as Fig. 3 has a meaning only for $\rho \geq r_g$.

宇宙空間のトポロジー

Burbidge　　　クエイサーの赤方Ｇｒａｖｉｔｙ偏移　ｚ　に　規則性

Fang-Sato　閉じた空間　１周、２周、３周、・・・

Gravity Award

方 励之
 科技大学学長､解雇､天安門事件､米大使館､米国^亡命

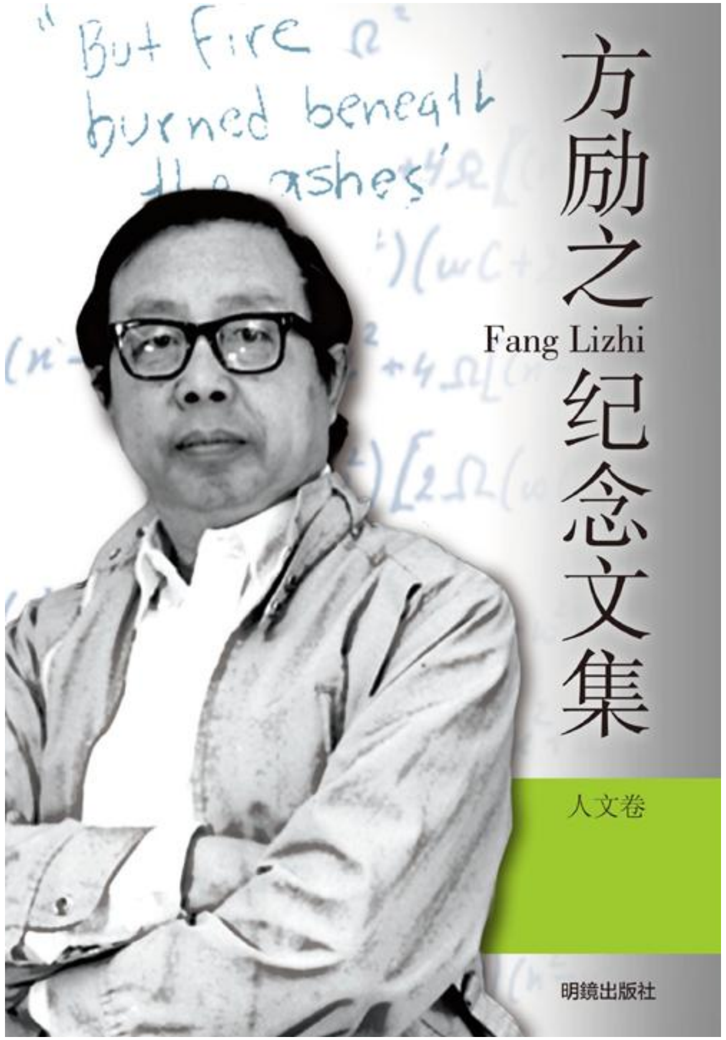

終わり

If we set in

$$\tanh U_0 = \tanh U_0^a = \frac{1-a_0^2}{1+a_0^2}, \quad c_0 = \frac{b_0 - a_0}{1+a_0 b_0}, \tag{5.13}$$

then, accordingly, a stationary two-Euclidean solution is constructed, which coincides with the Kerr-NUT solution in form:

$$f = f^0_{2,-,+} = \frac{k_o(xy-1) + k_o(x-y)\tanh U(x,y,a_0,b_0)}{f^0_{1,+}} = \frac{A_2}{B_2},$$

$$\Phi = \Phi^0_{2,-,+} = \frac{k_0}{f^0_{1,+}} \cdot \frac{(x-y)}{\cosh U(x,y,a_0,b_0)} + \omega^0_{1,+} = \frac{C_2}{B_2},$$

$$A_2 = (x^2-1)(1+a_0 b_0)^2 + (y^2-1)(b_0-a_0)^2,$$

$$B_2 = \left[(1+a_0 b_0)x + (1-a_0 b_0)\right]^2 + \left[(b_0-a_0)y + (b_0+a_0)\right]^2, \tag{5.14}$$

$$C_2 = 2\left[(b_0+a_0)(1+a_0 b_0)x - (b_0-a_0)(1-a_0 b_0)y\right].$$

If we set $a_0 = -b_0$, then (5.14) yields the Kerr solution.

7 Three- und four- stationary euclidon solution

1-I. Let us consider superposition (6.3) of the stationary two-euclidon solution (6.2) whith the stationary own-euclidon solution $(f^0_{1,-},\ \ \Phi^0_{1,-})$.

This stationary three-euclidon solution is easy to rewrite as

$$f = f^0_{3,-,+,-} = \frac{k_0(xy-1) + k_0(x-y)\tanh U(a,b)}{f^0_{2,+,-}}, \tag{7.1}$$

$$\Phi = \Phi^0_{3,-,+,-} = \frac{1}{f^0_{2,+,-}} \cdot \frac{k_0(x-y)}{\cosh U(a,b)} + \omega^0_{2,+,-}, \tag{7.2}$$

where

$$f^0_{2,+,-} = \frac{k_0(xy+1) + k_0(x+y)\tanh U^a}{f^0_{1,-}}, \tag{7.3}$$

$$\omega^0_{2,+,-} = f^0_{1,-}\frac{(x+y)}{xy+1+(x+y)\cdot\tanh U^a} \cdot \frac{1}{\cosh U^a} + \Phi^0_{1,-}.$$

１ ９ ８ ５年

In order to make a nonlinear "composition" of the solution (4.2) with the seed solution, we use the method of variation of parameters. We shall consider C_1, C_2, C_3 and U_0 in the solution (4.2) to be functions

$$C_1 \to f^0(\rho, z), \quad C_2 \to \omega^0(\rho, z), \quad C_3 \to \Phi^0(\rho, z), \quad U_0 \to U(\rho, z). \tag{4.3}$$

In this case we have

$$f = \frac{(z - z_1) + \sqrt{\rho^2 + (z - z_1)^2}\tanh U(\rho, z)}{f^0},$$

$$\Phi = \frac{\sqrt{\rho^2 + (z - z_1)^2}}{f^0 \cdot \cosh U(\rho, z)} + \omega^0(\rho, z),$$

$$\omega = f^0 \frac{\sqrt{\rho^2 + (z - z_1)^2}}{(z - z_1) + \sqrt{\rho^2 + (z - z_1)^2}\tanh U(\rho, z)} \cdot \frac{1}{\cosh U(\rho, z)} + \tag{4.4}$$

$$+\Phi^0(\rho, z).$$

1-I. If we choose

$$f^0 = 1, \quad \Phi^0 = \omega^0 = 0, \tag{5.7}$$

in this case we obtain from

$$f = f^0_{1,-} = k_0(xy-1) + k_0(x-y)\tanh U_0, \quad \Phi = \Phi^0_{1,-} = \frac{k_0(x-y)}{\cosh U_0}, \tag{5.8}$$

$$\omega = \frac{(x-y)}{xy-1+(x-y)\tanh U_0}\frac{1}{\cosh U_0},$$

where $U = U_{1,-} = U_0$.

1-II. If we choose

$$f^0 = f^0_{1,-}, \quad \Phi^0 = \Phi^0_{1,-}, \tag{5.9}$$

in this case we obtain from

$$f = f^0_{2,-,-} = \frac{k_o(xy-1) + k_o(x-y)\tanh U}{f^0_{1,-}}, \quad \Phi = \Phi^0_{2,-,-} = \frac{k_0}{f^0_{1,-}}\frac{(x-y)}{\cosh U} + \omega^0_{1,-},$$

where $U = U_{2,-,-} = \ln\frac{a}{b} = const$,

$$\frac{a}{b} = -\sqrt{\frac{1+\tanh U_0}{1-\tanh U_0}}, \quad \tanh U = \tanh U_0, \quad \cosh U = -\cosh U_0,$$

and

$$f = f^0_{2,-,-} = 1, \quad \Phi = \omega = 0. \tag{5.10}$$

$$f^0 = f^0_{1,+} = k_0(xy+1) + k_0(x+y)\tanh U_0, \quad \Phi^0 = \Phi^0_{1,+} = \frac{k_0(x+y)}{\cosh U_0}, \tag{5.11}$$

$$\omega^0 = \omega^0_{1,+} = \frac{(x+y)}{xy+1+(x+y)\cdot\tanh U_0} \cdot \frac{1}{\cosh U_0}$$